Spring 5-15-2016

Feed-forward Inhibitory Circuits in Hippocampus and Their Computational Role in Fragile X Syndrome

Sarah Lauren Wahlstrom Helgren
Washington University in St. Louis

WASHINGTON UNIVERSITY IN ST. LOUIS

School of Engineering & Applied Science
Department of Biomedical Engineering

Dissertation Examination Committee:
Vitaly Klyachko, Chair
Bruce Carlson
James Heuttner
Tim Holy
Steve Mennerick
Barani Raman
Kurt Thoroughman

Feed-forward Inhibitory Circuits in Hippocampus and Their Computational Role in Fragile X Syndrome

by

Sarah Wahlstrom Helgren

A dissertation presented to the
Graduate School of Arts & Sciences
of Washington University in
partial fulfillment of the
requirements for the degree
of Doctor of Philosophy

May 2016
St. Louis, Missouri

Table of Contents

List of Figures

Acknowledgments

I would like to thank my mentor, Vitaly Klyachko, for all of his support, training, patience, and everyday persistence in my pursuit of my PhD and a career in science. Additionally, I would to thank the members of the Klyachko lab, both past and present, as well as my husband and family.

I would also like to thank my funding sources both the grant to Vitaly Klyachko from the NINDS R01 NS081972, and the Cognitive, Computational, and Systems Neuroscience pathway IGERT pre-doctoral fellowship I received.

Sarah Wahlstrom Helgren

Washington University in St. Louis

May 2016

Dedicated to my parents.

ABSTRACT OF THE DISSERTATION

Feed-forward Inhibitory Circuits in the Hippocampus and Their Computational Role in Fragile X Syndrome

by

Sarah Wahlstrom Helgren

Doctor of Philosophy in Biomedical Engineering

Washington University in St. Louis, 2016

Professor Vitaly Klyachko, Chair

Feed-forward inhibitory (FFI) circuits are canonical neural microcircuits. They are unique in that they are comprised of excitation rapidly followed by a time-locked inhibition. This sequence provides for a powerful computational tool, but also a challenge in the analysis and study of these circuits. In this work, mechanisms and computations of two hippocampal FFI circuits have been examined. Specifically, the modulation of synaptic strength of the excitation and the inhibition is studied during constant-frequency and naturalistic stimulus patterns to reveal how FFI circuit properties and operations are dynamically modulated during ongoing activity. In the first part, the FFI circuit dysfunction in the mouse model of Fragile X syndrome, the leading genetic cause of autism, is explored. The balance between excitation and inhibition is found to be markedly abnormal in the *Fmr1* KO mouse, leading to failure of FFI circuit to perform spike modulation tasks properly. The mechanisms underlying FFI circuit dysfunction are explored and a critical role of presynaptic $GABA_B$ receptors is revealed. Specifically,

excessive presynaptic GABA receptor signaling is found to suppress GABA release in a subset of hippocampal interneurons leading to excitation/inhibition imbalance. In the second part, the dynamic changes during input bursts are explored both experimentally and in a simulated circuit. Because of the short-term synaptic plasticity of individual circuit components, the burst is found to play an important role in the modulating precision of the output cell spiking. The role of dynamics balance of excitation and inhibition during bursts in output spiking precision is further explored. Overall, the balance of excitation and inhibition is found to be critical for FFI circuit performance.

Chapter 1: Background

This chapter is intended to prepare the reader with the needed background material to understand the work in the following chapters. The sections on feed-forward inhibition and Fragile X Syndrome are to provide understanding of the previous work in these fields. The hippocampus is the system where this is studied in this work, so the basic background information on it is provided.

1.1 Feed-Forward Inhibitory Circuits

There are two canonical unitary microcircuits found throughout the brain, feed-forward inhibitory (FFI) and feedback inhibitory (FBI) circuits. Much like chips on a breadboard, these two components are assembled in a complex architecture that allows for the functional tasks of various brain regions to be carried out. By understanding the behavior and underlying mechanisms of the canonical microcircuits, a better understanding of the local network operations can be achieved. Whether a circuit is feed-forward or feedback depends on the synaptic connectivity, whereas, whether the circuit is excitatory or inhibitory depends on the neurotransmitter identity of the synapses and corresponding receptors.

The focus of my studies is on the FFI circuit. FFI circuits are found in various areas throughout the brain, such as, hippocampus (Klyachko & Stevens, 2006; F Pouille & Scanziani, 2001), the somatosensory cortex (Gabernet, Jadhav, Feldman, Carandini, & Scanziani, 2005), and in LGN (Blitz & Regehr, 2005). The FFI circuit is particularly interesting because of its unique computational potential. In this circuit the excitatory input drives the target post-synaptic cell, as well as an inhibitory interneuron. That interneuron then in turn inhibits the same post-synaptic cell. Together this results in a feed-forward inhibition. The key feature of the FFI

circuits is a time-locked inhibition that rapidly follows excitation within only 1-2 milliseconds making this circuit a computationally powerful circuit unit.

One important computational role of FFI circuit is the regulation of the size of the coincidence detection window. When two inputs are converging onto the same post-synaptic cell, they must be close in time in order to have the resulting excitatory-post-synaptic potentials (EPSPs) summate effectively for the target cell to cross the threshold for spiking (Pouille & Scanziani, 2001). FFI narrows the width of an incoming EPSP (Turner, 1990). Therefore, in the presence of FFI, the window of time for the two inputs to coincide becomes narrower than in the absence of FFI (Pouille & Scanziani, 2001). Additionally, in the presence of two input stimuli, FFI circuits are well-suited for order-selectivity computations (Goudar & Buonomano, 2015).

FFI circuits also play a critical role in processing of incoming spike bursts. Bursting is a common spiking behavior of many principle neurons in the brain (Izhikevich, 2010). For example, in the case of hippocampal circuit, spike bursts of pyramidal CA3 and CA1 neurons serve to carry information about an animal's position in the environment, known as place cell discharges (Moser, Kropff, & Moser, 2008). In this case, the FFI circuit processing becomes more complex as the short-term plasticity (STP) rapidly modulates properties of the synapses involved. In the excitatory synapse, there is a facilitation during bursts increasing the synaptic strength of the excitation. Whereas, in the inhibitory synapse, there is typically a depression in the synaptic strength causing a decrease in the inhibition during bursts. These two coinciding changes in gain, which amplitude is dependent on the frequency of the burst, create a simple high-pass filter (Klyachko & Stevens, 2006) that causes the increase in the magnitude of the EPSCs in the target neuron selectively at higher frequencies (Klyachko & Stevens, 2006).

On a population level, the FFI circuit is computationally critical for the expansion of the cortical dynamic range. Thus, for a stimulus of weak intensity, only a few cells will respond, and it would take a very large stimulus to make the entire population of cells respond. In the absence of FFI, the difference in stimulus intensity needed to go from few cells responding to all the cells of the population responding is one fourth of the change needed in the presence of FFI circuits (Frédéric Pouille, Marin-Burgin, Adesnik, Atallah, & Scanziani, 2009). Thus, the input intensity can modulate the size of the population response with greater precision because of the presence of FFI circuits.

The role of FFI is not limited to somatic computation. FFI is also important for restricting the spread of depolarization within the dendritic tree (Willadt, Nenniger, & Vogt, 2013). This is critical for limiting the spatial integration of signals that occurs in the dendrites.

Although much is known about FFI circuits, there are many remaining questions. Because each synapse within the circuit undergoes rapid dynamic changes, how these circuits operate during complex natural circuit activity remains largely unexplored. Furthermore, there is little understanding about changes in these circuits in disease states when the synaptic dynamics and the balance of excitation and inhibition are abnormal.

1.2 Hippocampus

The hippocampus is a cortical brain structure. It is known for its critical role in learning, memory, and navigation. Most of the early work of understanding the role and importance of hippocampus comes from patient H.M. whose hippocampus was removed to prevent seizures and from recordings of hippocampal place cells (Buzsáki & Moser, 2013).

1.2.1 Regions of the Hippocampus

The hippocampus is one of the oldest anatomical brain structures. It consists of three distinct regions—cornu ammonis 1 (CA1), CA2, and CA3. The dentate gyrus (DG) is also often included in the description of the hippocampus, however, it is technically apart of the hippocampal formation and not the hippocampus proper (Anderson, Morris, Amaral, Bliss, & O'Keefe, 2006). The CA1, CA2 and CA3 regions of the hippocampus all consist, like most of cortex, of a dominate pyramidal cell layer which receives inputs from the adjacent regions and from other brain structures. The surrounding layers of each region are then filled with critical interneurons forming local circuits. The DG is a unique region of the hippocampus, made up primarily of granule cells (Anderson et al., 2006). The CA3 region of the hippocampus is well-studied and is unique because many CA3 pyramidal cells project onto other CA3 cells forming associational connections (Anderson et al., 2006). The pyramidal cells in this region are also known to be so called place cells that respond with elevated firing to specific locations in the animal's environment. The CA2 region of the hippocampus was largely ignored for many years, but recently has been found to play a critical role specifically in social memory (Hitti & Siegelbaum, 2014).

The CA1 region of hippocampus is the most studied. It is known to contain place cells. The pyramidal cells in this region receive two distinct inputs from the tri-synaptic pathway (described in detail below) and the perforant path input from the cortical layer 3 at the proximal and distal dendrites respectively. Unlike CA3, the CA1 region has limited associational connections (Anderson et al., 2006). It also makes projections out of the hippocampus proper to the subiculum.

1.2.2 The Tri-Synaptic Pathway

The tri-synaptic pathway originates in layer II of the enthorhinal cortex. It innervates the dentate gyrus, then CA3, and finally, the proximal dendrites of the CA1 pyramidal cells in the stratum radiatum layer. It should also be noted that there are axons from CA3 that project to the stratum oriens of the CA1 region (Anderson et al., 2006). This is a primarily uni-directional pathway (Anderson et al., 2006). The portion of this pathway that connects the CA3 region to the CA1 region is referred to as the Schaffer Collateral (SC) pathway. This pathway is thought to play a role in the orthogonalization of incoming data, and thus, allows for the storage of associations with minimal interference (Buzsáki & Moser, 2013).

1.2.3 The Perforant Path

The perforant path originates in the enthorhinal cortex. The fibers that branch off in the CA1 region along what is known as the Temporoammonic (TA) pathway originate in layer III of the enthorhinal cortex (Anderson et al., 2006). In CA1, the TA pathway synapses onto the distal dendrites of the CA1 pyramidal cells in stratum lacunosum-moleculare layer. The perforant path also continues on to synapse at the distal dendrites of the CA2 and CA3 pyramidal cells. A study of mice where this pathway has been inhibited indicates that this pathway is involved in the temporal association memory formation (Suh, Rivest, Nakashiba, Tominaga, & Tonegawa, 2011).

1.3 Fragile X Syndrome

Neural circuit dysfunction is common feature of many neurodevelopmental disorders, including autism spectrum disorders, Down Syndrome, and schizophrenia (Gibson, Bartley, Hays, & Huber, 2008; Gonçalves, Anstey, Golshani, & Portera-Cailliau, 2013; Kleschevnikov et al., 2012; Pollard et al., 2012). Among these, Fragile X Syndrome (FXS) is the most common

genetic cause of intellectual disability and autism. FXS is a chromosomal abnormality caused by more than 200 repeats of the trinucleotide (CGG) in the 5' untranslated region of the *FMR1* gene (Mailick et al., 2014). This mutation causes transcriptional silencing of the Fragile X Mental Retardation Protein (FMRP). FMRP is known to be involved in RNA-binding, as a regulator of protein synthesis, with downstream effects on synaptic development and plasticity (Mailick et al., 2014). Despite extensive efforts, how loss of FMRP causes the multiple devastating behavioral and intellectual disability symptoms is poorly understood. The primary tool for studying FXS is the use of *Fmr1* knock out (KO) mice that reproduce well the FXS phenotypes at the structural, synaptic and circuit levels (Contractor, Klyachko, & Portera-Cailliau, 2015).

1.3.1 Previous Work on FXS

Much of the early work on FXS has focused on long-term changes in the post-synaptic dendrites. In hippocampal and cortical synapses, some forms of long-term depression (LTD) have been shown to be significantly enhanced in *Fmr1* knock out mice (Bear, Huber, & Warren, 2004). LTD can be induced in multiple ways, including by the post-synaptic activation of mGluRs, specifically, mGluR1 and mGluR5 (Bear et al., 2004). From this, the hypothesis arose, known as mGluR theory of FXS that the use of mGluR antagonists could be used to reverse the fragile X phenotypes (Bear et al., 2004). However, multiple recent clinical trials of different mGluR antagonists failed to produce significant improvements in either adolescents or in adults (Mullard, 2015).

1.3.2 Hyperexcitability in Fragile X Syndrome

Although much of the work on FXS has focused on changes seen in the hippocampus, it is important to note that many other brain regions show significant changes in the disease state. This includes the accumbens where in *Fmr1* knock out mice changes in both structure and

function have been shown (Neuhofer et al., 2015). Also, in the amygdala, GABAergic synaptic transmission is reduced in *Fmr1* KO mice (Martin, Corbin, & Huntsman, 2014). In the auditory brainstem, a decreased cell size and over-expression of vesicular GABA transporter protein (VGAT) has been shown in *Fmr1* KO mice (Rotschafer, Marshak, & Cramer, 2015). Interestingly, there has been little consistency of changes between different brain regions. However, by looking across these regions and the symptom of seizures that many FXS patients suffer from, a general theme has started to emerge of a hyperexcitability that results from an imbalance in excitation and inhibition in FXS circuits. Such hyperexcitability can be the result of too much excitation or too little inhibition, or both. Yet the mechanisms underlying circuit defects in FXS and excitation\inhibition imbalance remain poorly understood.

In the hippocampus, circuit hyperexcitability has also been described. Specifically, in the SC pathway, excitatory synapses have been shown to have an elevated glutamate release during high-frequency activity, and natural stimulation due to abnormally increased short-term augmentation (Deng, Sojka, & Klyachko, 2011). This defect is caused by a reduced activity of one type of K+ channels, called the large conductance calcium-activated (BK) channels (Deng et al., 2013). The reduced activity of these BK channels leads to a prolonged action potential width and an increased Ca^{2+} influx into the presynaptic terminal (Deng et al., 2013) leading in turn to elevated glutamate release specifically during high-frequency bursts. Unlike excitation, defects in inhibition has been studied to a much lesser degree in hippocampus of Fmr1 KO mice and across brain regions. One study showed that in FXS patients, $GABA_A$ receptors are reduced (D'Hulst et al., 2015). Additionally, the role of endocannabinoids at GABAergic synapses has been indicated as a source of decreased inhibition in hippocampus (Tang & Alger, 2015). Although, both excitation and inhibition have been studied independently in FXS, how the

imbalance between excitation and inhibition contributes to circuit defects in this disorder and the resulting changes in the computational circuit operations remains largely unexplored.

References

Anderson, P., Morris, R., Amaral, D., Bliss, T., & O'Keefe, J. (2006). *The Hippocampus Book*. Oxford Scholarship Online. Retrieved from http://www.oxfordscholarship.com/view/10.1093/acprof:oso/9780195100273.001.0001/acprof-9780195100273-chapter-3?print

Ang, C. W., Carlson, G. C., & Coulter, D. a. (2005). Hippocampal CA1 circuitry dynamically gates direct cortical inputs preferentially at theta frequencies. *Journal of Neuroscience*, *25*(42), 9567–80. doi:10.1523/JNEUROSCI.2992-05.2005

Bartley, A. F., & Dobrunz, L. E. (2015). Short-term plasticity regulates the excitation / inhibition ratio and the temporal window for spike integration in CA1 pyramidal cells. *European Journal of Neuroscience*, *41*(February), 1402–1415. doi:10.1111/ejn.12898

Bear, M. F., Huber, K. M., & Warren, S. T. (2004). The mGluR theory of fragile X mental retardation. *Trends in Neurosciences*, *27*(7), 370–377. doi:10.1016/j.tins.2004.04.009

Blitz, D. M., & Regehr, W. G. (2005). Timing and specificity of feed-forward inhibition within the LGN. *Neuron*, *45*(6), 917–28. doi:10.1016/j.neuron.2005.01.033

Brager, D. H., & Johnston, D. (2014). Channelopathies and dendritic dysfunction in fragile X syndrome. *Brain Research Bulletin*, *103*, 11–17. doi:10.1016/j.brainresbull.2014.01.002

Buzsáki, G., & Moser, E. I. (2013). Memory, navigation and theta rhythm in the hippocampal-entorhinal system. *Nature Neuroscience*, *16*(2), 130–8. doi:10.1038/nn.3304

Chittajallu, R., Pelkey, K. A., & McBain, C. J. (2013). Neurogliaform cells dynamically regulate somatosensory integration via synapse-specific modulation. *Nature Neuroscience*, *16*(1), 13–15. doi:10.1038/nn.3284

Contractor, A., Klyachko, V. A., & Portera-Cailliau, C. (2015). Altered Neuronal and Circuit Excitability in Fragile X Syndrome. *Neuron*, *87*(4), 699–715. doi:10.1016/j.neuron.2015.06.017

D'Hulst, C., Heulens, I., Van der Aa, N., Goffin, K., Koole, M., Porke, K., … Kooy, R. F. (2015). Positron Emission Tomography (PET) Quantification of GABAA Receptors in the Brain of Fragile X Patients. *Plos One*, *10*(7), e0131486. doi:10.1371/journal.pone.0131486

Deng, P., & Klyachko, V. A. (2015). Genetic Upregulation of BK Channel Activity Normalizes Multiple Synaptic and Circuit Defects in a Mouse Model of Fragile X Syndrome Departments of Cell Biology and Physiology , Biomedical Engineering , CIMED , Washington University , St . Louis , MO ; *Journal of Physiology*, 0–26.

doi:10.1113/JP271031.This

Deng, P., Rotman, Z., Blundon, J. a, Cho, Y., Cui, J., Cavalli, V., … Klyachko, V. a. (2013). FMRP regulates neurotransmitter release and synaptic information transmission by modulating action potential duration via BK channels. *Neuron*, *77*(4), 696–711. doi:10.1016/j.neuron.2012.12.018

Deng, P., Sojka, D., & Klyachko, V. a. (2011). Abnormal Presynaptic Short-Term Plasticity and Information Processing in a Mouse Model of Fragile X Syndrome. *Journal of Neuroscience*, *31*(30), 10971–10982. doi:10.1523/JNEUROSCI.2021-11.2011

Ferrante, M., Migliore, M., & Ascoli, G. a. (2009). Feed-forward inhibition as a buffer of the neuronal input-output relation. *Proceedings of the National Academy of Sciences of the United States of America*, *106*(42), 18004–9. doi:10.1073/pnas.0904784106

Gabernet, L., Jadhav, S. P., Feldman, D. E., Carandini, M., & Scanziani, M. (2005). Somatosensory Integration Controlled by Dynamic Thalamocortical Feed-Forward Inhibition. *Neuron*, *48*(2), 315–327. doi:10.1016/j.neuron.2005.09.022

Garner, C., & Wetmore, D. (2012). Synaptic Plasticity (Vol. 970, pp. 553–572). doi:10.1007/978-3-7091-0932-8

George, A. a, Lyons-Warren, A. M., Ma, X., & Carlson, B. a. (2011). A diversity of synaptic filters are created by temporal summation of excitation and inhibition. *The Journal of Neuroscience : The Official Journal of the Society for Neuroscience*, *31*(41), 14721–34. doi:10.1523/JNEUROSCI.1424-11.2011

Gibson, J. R., Bartley, A. F., Hays, S. a, & Huber, K. M. (2008). Imbalance of neocortical excitation and inhibition and altered UP states reflect network hyperexcitability in the mouse model of fragile X syndrome. *Journal of Neurophysiology*, *100*(5), 2615–26. doi:10.1152/jn.90752.2008

Gonçalves, J. T., Anstey, J. E., Golshani, P., & Portera-Cailliau, C. (2013). Circuit level defects in the developing neocortex of Fragile X mice. *Nature Neuroscience*, *16*(7), 903–909. doi:10.1038/nn.3415

Goudar, V., & Buonomano, D. V. (2015). A model of order-selectivity based on dynamic changes in the balance of excitation and inhibition produced by short-term synaptic plasticity. *Journal of Neurophysiology*, *113*(2), 509–523. doi:10.1152/jn.00568.2014

Hennig, M. H. (2013). Theoretical models of synaptic short term plasticity. *Frontiers in Computational Neuroscience*, *7*(April), 45. doi:10.3389/fncom.2013.00045

Hitti, F. L., & Siegelbaum, S. a. (2014). The hippocampal CA2 region is essential for social memory. *Nature*, *508*(7494), 88–92. doi:10.1038/nature13028

Izhikevich, E. (2010). *Dynamical Systems in Neuroscience*. Cambridge, MA: MIT Press.

Izumi, Y., & Zorumski, C. F. (2008). Direct cortical inputs erase long-term potentiation at Schaffer collateral synapses. *The Journal of Neuroscience : The Official Journal of the Society for Neuroscience*, *28*(38), 9557–63. doi:10.1523/JNEUROSCI.3346-08.2008

Jang, H. J., & Kwag, J. (2012). GABAA receptor-mediated feedforward and feedback inhibition differentially modulate hippocampal spike timing-dependent plasticity. *Biochemical and Biophysical Research Communications*, *427*(3), 466–72. doi:10.1016/j.bbrc.2012.08.081

Kandaswamy, U., Deng, P.-Y., Stevens, C. F., & Klyachko, V. a. (2010). The role of presynaptic dynamics in processing of natural spike trains in hippocampal synapses. *The Journal of Neuroscience : The Official Journal of the Society for Neuroscience*, *30*(47), 15904–14. doi:10.1523/JNEUROSCI.4050-10.2010

Keck, C., Savin, C., & Lücke, J. (2012). Feedforward inhibition and synaptic scaling--two sides of the same coin? *PLoS Computational Biology*, *8*(3), e1002432. doi:10.1371/journal.pcbi.1002432

Kleschevnikov, A. M., Belichenko, P. V, Faizi, M., Jacobs, L. F., Htun, K., Shamloo, M., & Mobley, W. C. (2012). Deficits in Cognition and Synaptic Plasticity in a Mouse Model of Down Syndrome Ameliorated by GABA B Receptor Antagonists, *32*(27), 9217–9227. doi:10.1523/JNEUROSCI.1673-12.2012

Klug, A., Borst, J. G. G., Carlson, B. A., Kopp-Scheinpflug, C., Klyachko, V. A., & Xu-Friedman, M. A. (2012). How Do Short-Term Changes at Synapses Fine-Tune Information Processing? *Journal of Neuroscience*, *32*(41), 14058–14063. doi:10.1523/JNEUROSCI.3348-12.2012

Klyachko, V. a, & Stevens, C. F. (2006). Excitatory and feed-forward inhibitory hippocampal synapses work synergistically as an adaptive filter of natural spike trains. *PLoS Biology*, *4*(7), e207. doi:10.1371/journal.pbio.0040207

König, P., Engel, A. K., Roelfsema, P. R., & Singer, W. (1996). Coincidence detection or temporal integration. The role of the cortical neuron revisited. *Trends Neurosci.*, *19*(4), 130–137.

LeBlanc, J. J., DeGregorio, G., Centofante, E., Vogel-Farley, V. K., Barnes, K., Kaufmann, W. E., … Nelson, C. A. (2015). Visual evoked potentials detect cortical processing deficits in Rett syndrome. *Annals of Neurology*, n/a–n/a. doi:10.1002/ana.24513

Mailick, M. R., Hong, J., Rathouz, P., Baker, M. W., Greenberg, J. S., Smith, L., & Maenner, M. (2014). Low-normal FMR1 CGG repeat length: phenotypic associations. *Frontiers in Genetics*, *5*(September), 1–8. doi:10.3389/fgene.2014.00309

Martin, B. S., Corbin, J. G., & Huntsman, M. M. (2014). Deficient tonic GABAergic conductance and synaptic balance in the Fragile-X Syndrome Amygdala. *Journal of Neurophysiology*, *3*(303), 890–902. doi:10.1152/jn.00597.2013

Moser, E. I., Kropff, E., & Moser, M.-B. (2008). Place cells, grid cells, and the brain's spatial representation system. *Annual Review of Neuroscience*, *31*, 69–89. doi:10.1146/annurev.neuro.31.061307.090723

Mullard, A. (2015). Fragile X disappointments upset autism ambitions. *Nature Reviews Drug Discovery*, *14*(3), 151–153. doi:10.1038/nrd4555

Neuhofer, D., Henstridge, C. M., Dudok, B., Sepers, M., Lassalle, O., Katona, I., & Manzoni, O. J. (2015). Functional and structural deficits at accumbens synapses in a mouse model of Fragile X. *Frontiers in Cellular Neuroscience*, *9*(March), 1–15. doi:10.3389/fncel.2015.00100

Pollard, M., Varin, C., Hrupka, B., Pemberton, D. J., Steckler, T., & Shaban, H. (2012). Synaptic transmission changes in fear memory circuits underlie key features of an animal model of schizophrenia. *Behavioural Brain Research*, *227*(1), 184–93. doi:10.1016/j.bbr.2011.10.050

Pouille, F., Marin-Burgin, A., Adesnik, H., Atallah, B. V, & Scanziani, M. (2009). Input normalization by global feedforward inhibition expands cortical dynamic range. *Nature Neuroscience*, *12*(12), 1577–85. doi:10.1038/nn.2441

Pouille, F., & Scanziani, M. (2001). Enforcement of temporal fidelity in pyramidal cells by somatic feed-forward inhibition. *Science (New York, N.Y.)*, *293*(5532), 1159–63. doi:10.1126/science.1060342

Remondes, M., & Schuman, E. M. (2002). Direct cortical input modulates plasticity and spiking in CA1 pyramidal neurons. *Nature*, *416*(6882), 736–40. doi:10.1038/416736a

Rieke, F., Warland, D., Steveninck, R., & Bialek, W. (1999). *Spikes*. Cambridge, MA: MIT Press.

Rotman, Z., Deng, P.-Y., & Klyachko, V. a. (2011). Short-Term Plasticity Optimizes Synaptic Information Transmission. *Journal of Neuroscience*, *31*(41), 14800–14809. doi:10.1523/JNEUROSCI.3231-11.2011

Rotschafer, S. E., Marshak, S., & Cramer, K. S. (2015). Deletion of Fmr1 Alters Function and Synaptic Inputs in the Auditory Brainstem. *Plos One*, *10*(2), e0117266. doi:10.1371/journal.pone.0117266

Rubenstein, J. L. R., & Merzenich, M. M. (2003). Model of autism: increased ratio of excitation/inhibition in key neural systems. *Genes, Brain, and Behavior*, *2*(5), 255–267. doi:10.1046/j.1601-183X.2003.00037.x

Saraga, F., Balena, T., Wolansky, T., Dickson, C. T., & Woodin, M. a. (2008). Inhibitory synaptic plasticity regulates pyramidal neuron spiking in the rodent hippocampus. *Neuroscience*, *155*(1), 64–75. doi:10.1016/j.neuroscience.2008.05.009

Schreiber, S., Fellous, J. M., Whitmer, D., Tiesinga, P., & Sejnowski, T. J. (2003). A new correlation-based measure of spike timing reliability. *Neurocomputing*, *52-54*, 925–931. doi:10.1016/S0925-2312(02)00838-X

Suh, J., Rivest, A. J., Nakashiba, T., Tominaga, T., & Tonegawa, S. (2011). Entorhinal Cortex Layer III Input to the Hippocampus Is Crucial for Temporal Association Memory. *Science (New York, N.Y.)*, (November). doi:10.1126/science.1210125

Tang, X. A., & Alger, B. E. (2015). Homer Protein – Metabotropic Glutamate Receptor Binding Regulates Endocannabinoid Signaling and Affects Hyperexcitability in a Mouse Model of Fragile X Syndrome, *35*(9), 3938–3945. doi:10.1523/JNEUROSCI.4499-14.2015

Tsay, D., Dudman, J. T., & Siegelbaum, S. a. (2007). HCN1 channels constrain synaptically evoked Ca2+ spikes in distal dendrites of CA1 pyramidal neurons. *Neuron*, *56*(6), 1076–89. doi:10.1016/j.neuron.2007.11.015

Turner, D. (1990). Feed-Forward Inhibitory Potentials and Excitatory Interactions in Guinea-Pig Hippocampal Pyramidal Cells. *Journal of Physiology*, *422*(1), 333–350.

Wahlstrom-Helgren, S., & Klyachko, V. A. (2015). GABA $_B$ receptor-mediated feed-forward circuit dysfunction in the mouse model of fragile X syndrome. *The Journal of Physiology*, doi:10.1113/JP271190

Willadt, S., Nenniger, M., & Vogt, K. E. (2013). Hippocampal Feedforward Inhibition Focuses Excitatory Synaptic Signals into Distinct Dendritic Compartments. *PLoS ONE*, *8*(11), e80984. doi:10.1371/journal.pone.0080984

Wlodarczyk, A. I., Xu, C., Song, I., Doronin, M., Wu, Y.-W., Walker, M. C., & Semyanov, A. (2013). Tonic GABAA conductance decreases membrane time constant and increases EPSP-spike precision in hippocampal pyramidal neurons. *Frontiers in Neural Circuits*, *7*(December), 205. doi:10.3389/fncir.2013.00205

Zalay, O. C., & Bardakjian, B. L. (2006). Simulated mossy fiber associated feedforward circuit functioning as a highpass filter. *Conference Proceedings : ... Annual International Conference of the IEEE Engineering in Medicine and Biology Society. IEEE Engineering in Medicine and Biology Society. Conference*, *1*, 4979–82. doi:10.1109/IEMBS.2006.260702

Zhou, M., Tao, H. W., & Zhang, L. I. (2012). Generation of intensity selectivity by differential synaptic tuning: fast-saturating excitation but slow-saturating inhibition. *The Journal of Neuroscience : The Official Journal of the Society for Neuroscience*, *32*(50), 18068–78.

doi:10.1523/JNEUROSCI.3647-12.2012

Chapter 2: $GABA_B$ Receptor-Mediated Feed-Forward Circuit Dysfunction in the Mouse Model of Fragile X Syndrome

This chapter was co-written by Sarah Wahlstrom Helgren and Vitaly Klyachko. It was published in the Journal of Physiology in 2015.

Circuit hyperexcitability has been implicated in neuropathology of Fragile X syndrome, the most common inheritable cause of intellectual disability. Yet, how canonical unitary circuits are affected in this disorder remains poorly understood. Here, we examined this question in the context of the canonical feed-forward inhibitory circuit formed by the Temporoammonic (TA) branch of the perforant path, the major cortical input to the hippocampus. TA feed-forward circuits exhibited a marked increase in excitation/inhibition ratio and major functional defects in spike modulation tasks in *Fmr1* KO mice, a Fragile X mouse model. Changes in feed-forward circuits were caused specifically by inhibitory, but not excitatory, synapse defects. TA-associated inhibitory synapses exhibited increase in paired-pulse ratio and in the coefficient of variation of IPSPs, consistent with decreased GABA release probability. TA-associated inhibitory synaptic transmission in *Fmr1* KO mice was also more sensitive to inhibition of $GABA_B$ receptors, suggesting an increase in presynaptic $GABA_B$ receptor ($GABA_BR$) signaling. Indeed, the differences in inhibitory synaptic transmission between *Fmr1* KO and WT mice were eliminated by a $GABA_BR$ antagonist. Inhibition of $GABA_BRs$ or selective activation of

presynaptic $GABA_BRs$ also abolished the differences in the TA feed-forward circuit properties between *Fmr1* KO and WT mice. These $GABA_BR$-mediated defects were circuit-specific and were not observed in the Schaffer collateral pathway-associated inhibitory synapses. Our results suggest that the inhibitory synapse dysfunction in the cortical-hippocampal pathway of *Fmr1* KO mice causes hyperexcitability and feed-forward circuit defects, which are mediated in part by a presynaptic $GABA_BR$-dependent reduction in GABA release.

2.1 Introduction

Loss of Fragile X mental retardation protein (FMRP) causes FXS, the leading genetic cause of mental disability, often associated with autism and seizures. The common seizure phenotype in FXS patients suggests a dysfunction in circuit excitability (Bassell and Warren, 2008), and many recent studies have implicated excitatory/inhibitory (E/I) imbalance in the pathophysiology of FXS (Paluszkiewicz et al., 2011). Circuit hyperexcitability has been observed in several brain areas of *Fmr1* KO mice, the mouse model of FXS, predominately at a network level (Gibson et al., 2008; Goncalves et al., 2013) and studies over the last decade uncovered a host of synaptic-level deficits in FXS models (Bassell and Warren, 2008). Yet, a large gap between these two levels of analysis limits further advances towards understanding and treatment of this disorder. Specifically, how fundamental unitary neural circuits are affected in FXS has not been examined.

Recent studies have implicated inhibitory synapse abnormalities as an important contributor to circuit excitability changes in FXS. Decreased excitatory drive onto inhibitory fast-spiking interneurons was observed in the cortex of *Fmr1* KO mice leading to a reduction in GABAergic transmission (Gibson et al., 2008). Consistent with these results, inhibitory synaptic transmission in the amygdala was reduced by FMRP loss (Olmos-Serrano et al., 2010). In contrast, evoked GABA release was unchanged in the subiculum (Curia et al., 2009), or even

increased in the striatum of *Fmr1* KO mice (Centonze et al., 2008). The direction and extent of the inhibitory synapse dysfunction caused by loss of FMRP thus remain debatable, and the mechanisms of circuit-level E/I imbalance in FXS remain incompletely understood.

Canonical feed-forward inhibitory (FFI) circuits provide a useful model system to study the E/I balance, since activation of these circuits result in excitation rapidly followed by time-locked inhibition (Pouille and Scanziani, 2001). FFI circuits represent the building blocks of higher-level circuitry and are essential for many fundamental information-processing tasks (Ang et al., 2005; Chittajallu et al., 2013; Dudman et al., 2007; Ferrante et al., 2009; Gabernet et al., 2005; Han and Heinemann, 2013; Izumi and Zorumski, 2008; Klyachko and Stevens, 2006; Pouille and Scanziani, 2001; Remondes and Schuman, 2004). Here, we examined the FFI circuit formed by a major cortical input to the hippocampus, the Temporoammonic (TA) branch of the perforant path. The CA1 region of the hippocampus integrates sensory inputs from the entorhinal cortex through the tri-synaptic pathway and directly from the entorhinal cortex via the TA pathway. These converging inputs to the hippocampus dynamically modulate each other via local inhibitory circuits (Remondes and Schuman, 2002). The FFI circuit of the TA pathway has been shown to be essential in a variety of tasks, including induction and modulation of many forms of synaptic plasticity (Dudman et al., 2007; Han and Heinemann, 2013; Izumi and Zorumski, 2008), maintenance of the hippocampal theta rhythm (Ang et al., 2005), and memory consolidation (Remondes and Schuman, 2004).

Here, we found that feed-forward inhibition is markedly diminished in the TA pathway of *Fmr1* KO mice, leading to an E/I circuit imbalance and abnormal FFI circuit functioning. These defects were associated specifically with the abnormalities in inhibitory, but not excitatory, synapse function. Our analyses are consistent with the predominate role of metabotropic

$GABA_B$ receptors in these defects, particularly an enhanced presynaptic $GABA_B$ receptor signaling in inhibitory synapses that suppresses GABA release in the absence of FMRP. Abnormal $GABA_B$ receptor signaling and altered GABA release thus play a major role in FFI circuit dysfunction in FXS.

2.2 Methods

Ethical Approval. All animal procedures conformed to the National Institute of Health guidelines and were approved by the Washington University Animal Studies Committee.

Animals and Slice Preparation. Fmr1 KO and WT control strain mice on FVB background were obtained from Jackson Laboratory (Bar Harbor, ME). Both male and female 18- to 23-day-old mice were used. Mice were fed *ad libitum*. Genotyping was performed according to the Jackson Laboratory protocols. Age-matched controls were used; our previous studies found littermate- and age-match controls to be indistinguishable in all measurements of both excitatory and inhibitory synaptic function (Deng et al., 2011, 2013, Myrick et al., 2015). Transverse hippocampal brain slices (350μm) were prepared using a microtome (Leica, Germany) in ice-cold ACSF containing: 125mM NaCl, 25mM $NaHCO_3$, 2.5mM KCl, 1.25mM NaH_2PO_4, 10mM glucose, 0.5mM CaCl2, 4.0mM $MgCl_2$. Slices were placed in a recovery chamber heated to 33°C for ~1hour, and then kept at room temperature (~23°C) until use.

Electrophysiology. All recordings were performed at 33-34°C in a bath solution containing the following: 125 mM NaCl, 25mM $NaHCO_3$, 2.50mM KCl, 1.25mM NaH_2PO_4, 10mM glucose, 2.0mM $CaCl_2$, 1.0mM $MgCl_2$, 50μM AP-5. Cell-attached or whole-cell recordings were made from CA1 pyramidal neurons visually identified with differential interference contrast optics

mounted on a Nikon E600N microscope and recorded using an Axopatch 200B amplifier (Molecular Devices). Synaptic responses were evoked by an extracellular monopolar electrode positioned on the TA branch of the perforant path in the hippocampal SLM layer. Care was taken to ensure that this simulation lead to specific activation of the FFI circuits of the TA pathway under our recording conditions: (i) an incision was made between the dentate gyrus and the CA3 areas to prevent activation of the tri-synaptic pathway by the TA stimulation; (ii) Analyses of the synaptic responses evoked in the same CA1 neuron by activation of the Schaffer collateral (SC) or the TA pathways indicated that FFI response in the SC pathway was over an order of magnitude smaller than the FFI response in the TA pathway under our recording conditions (Fig. 2); (iii) Defects in inhibitory synaptic transmission in the hippocampus of *Fmr1* KO mice were specific to inhibition evoked by the TA pathway stimulation, while inhibition associated with the SC pathway activation was not significantly different from WT (Fig. 2.8) as we reported previously (Deng et al., 2011); (iv) Excitatory component of the FFI circuit was normal in the TA pathway of *Fmr1* KO mice, while this component exhibited marked defects in the SC pathway (Deng et al., 2011; Deng et al., 2013; Wang et al., 2014). Our measurements of the FFI circuit of the TA pathway therefore were not contaminated by significant SC activation.

The recording electrodes were filled with solution containing (in mM): 130 K-gluconate, 10 KCl, 0.5 EGTA, 2 $MgCl_2$, 9 NaCl, 3 MgATP, 0.3 LiGTP, and 10 HEPES (pH 7.3). Custom software written in LabView in conjunction with a National Instruments A/D board was used to filter (at 2kHz) and digitize (at 20kHz) the signal. Because some heterogeneity exists in the CA1 pyramidal cell layer, additional care was taken to ensure that only recordings from pyramidal cells were considered for analysis. Upon establishing of whole-cell recording, a 1-sec-long depolarizing step was applied to evoke spiking. The frequency, height, width, hyperpolarization,

and adaptation of evoked action potentials (APs) were analyzed to determine if the cells qualified as pyramidal cells. In order to be considered a healthy pyramidal neuron, the APs must have satisfied the following criteria: >80mV in height, <2.5ms in full width at half maximum (FWHM), and have a spike frequency <50Hz. This analysis was performed in ~80% of all recorded cells. Of the 108 cells tested, 15 were rejected from further analysis based on these criteria. Accepted cells had an average AP height of 101.6±10.4mV, width of 1.12±0.19ms, frequency of 20.83±7.85Hz (mean ± S.D). All measurements were repeated multiple times in the same neuron with adequate recovery time between the trials. In addition, cells that had an EPSP peak less than the RMS of the baseline noise were excluded from I/E ratio analysis only. This was the case for 13 WT and 4 *Fmr1* KO neurons.

For basal FFI circuit measurements, responses were averaged across 10-20 repetitions per cell. The peak and time to peak of EPSP and IPSP components, and the FWHM of the EPSP were determined. In measurements of isolated excitatory responses, a traditional template analysis was used for high-frequency train measurements as described (Deng et al., 2011). Briefly, the template of baseline current was created by averaging of all baseline responses for a given cell. The template was then scaled to the current peak value following each stimulus and subtracted before the analysis of the sequential stimulus to remove contributions from overlapping responses. In measurements of isolated inhibitory responses during spike trains, a traditional template analysis on a train of stimuli could not be used because two components of response, $GABA_AR$- and $GABA_BR$-mediated, were present, each with independent dynamics. Instead, a minimum potential from the baseline following each stimulus was calculated and normalized to the average minimum value of the responses to single stimuli for the same cell. For Yh:Yd measurements, Yh was measured as the amount of decay that occurs from the peak of

excitation following a stimulus to the time just before the next stimulus occurs, while Yd was determined as the peak of excitation relative to the resting potential following a stimulus.

To determine an inhibitory paired-pulse ratio (PPR), we measured the slope of the first response from 20% to 80% of the peak. We then subtracted a scaled template created from the single stimulus responses before examining the slope of the second IPSP. Three *Fmr1* KO cells were excluded from this analysis because they did not contain an early IPSP that was detectable above the noise. Slope was chosen for this analysis to minimize the contribution of the late $GABA_BR$-dependent component, which does not reflect presynaptic changes.

Spike modulation experiments. Spike modulation measurements were performed in a cell-attached configuration. Bath solution was the same as above for whole-cell measurements; and was also used to fill the recording electrodes. SC stimulation intensity was determined by performing 30-50 single stimuli trials at 0.1Hz to evoke a spike in 10% of the trials (for spike enhancement experiments) or 90% of the trials (for spike blocking experiments). TA pathway was stimulated with a train of 10 spikes at 100Hz; the TA stimulus intensity was set to be below the threshold for evoking a spike in the target CA neuron by the TA pathway train alone, but strong enough to alter the SC evoked response when the two pathways were activated simultaneously. This effectively limits the intensity of TA stimulation to a narrow range. We note that these stimulation paradigms were designed to minimize slice-to-slice variability in setting stimulation intensity of the TA pathway, since no independent normalization factor for TA stimulus intensity could be used in these experiments. Indeed we ensured that no significant bias in setting stimulus intensity was present in our measurements by performing both spike enhancement and blocking experiments in the same slices in the majority of experiments. While SC intensity was adjusted accordingly, the TA stimulation intensity remained unaltered for the

spike enhancement and blocking experiments performed in the same cell. The opposite direction of changes in *Fmr1* KO mice in spike enhancement and spike blocking measurements (increase in spike enhancement, decrease in spike blocking) argues against a significant systematic bias in TA stimulus intensity because such bias would be expected to cause changes in the same direction in both measurements. We note that fEPSP cannot be used in these measurements as a normalization factor because it is intrinsically different in *Fmr1* KO and WT mice. The same TA stimulus intensity evokes larger fEPSP in *Fmr1* KO than WT animals because of reduced inhibition. Using the fEPSP as a normalization factor would therefore artificially remove differences between genotypes rather than provide a proper normalization for stimulus intensity. The same argument holds for the SC-pathway, except in this case fEPSP is larger in *Fmr1* KO mice for the same stimulus intensity because excitatory transmission is abnormally enhanced as we found previously (Deng et al., 2011, 2013).

Statistical Analysis. All statistical analyses were performed using MatLab. A non-parametric, two-sided, Wilcoxon rank sum test (also known as Mann-Whitney U test) was employed to compare between groups. Significance was assumed for $p<0.05$ (noted by *), values of $p<0.01$ and $p<0.001$ were noted by ** and *** respectively. The values expressed are mean ± S.E.M.

2.3 Results

2.3.1 Baseline feed-forward inhibition is diminished in Fmr1 KO mice

Abnormal circuit excitability has been described in *Fmr1* KO mice, predominately at a network level (Gibson et al., 2008; Goncalves et al., 2013), while the basic FFI circuits have not yet been examined. Therefore, we first examined whether the loss of FMRP affects the E/I balance in the

FFI circuit formed by the TA pathway, the major cortical input to the hippocampus. CA1 pyramidal neurons were current-clamped in whole-cell configuration and the activity in the FFI circuit was induced by a stimulus electrode placed on the TA pathway in the SLM layer (schematic in Fig. 2.1A). We note that this stimulation did not activate a measurable FFI response of the SC pathway under conditions of our recordings (Fig. 2.2 and see Methods for details) and therefore activated the FFI circuit of the TA pathway in a selective manner. To study the E/I balance we began by examining post-synaptic responses to a single stimulus of the TA pathway (Fig. 2.1B), which resulted in a canonical EPSP/IPSP sequence typical of an FFI circuit (Pouille and Scanziani, 2001; Remondes and Schuman, 2002). We found that the ratio of EPSP/IPSP peak values was markedly increased in this FFI circuit in *Fmr1* KO relative to WT mice (Fig. 2.1C, WT: 0.41 ± 0.61, $n = 34$; KO: 2.78 ± 0.18, $n = 42$; $p = 0.009$, Mann-Whitney U test, here and throughout). To make sure that these changes were not due to small apparent IPSP peak values in *Fmr1* KO mice, we also quantified the inverse, IPSP/EPSP ratio and found it to be significant reduced in *Fmr1* KO relative to WT mice (Fig. 2.1D, WT: 1.49 ± 0.16, $n = 34$; KO: 0.76 ± 0.07, $n = 42$; $p = 0.03$). EPSP duration was also significantly prolonged in the *Fmr1* KO neurons (Fig. 2.1E, full-width at half-maximum (FWHM) in WT: 19.3 ± 0.86 ms, in KO: 24.0 ± 0.65 ms, $p = 0.02$), consistent with reduced FFI (Pouille and Scanziani, 2001). No significant changes were observed in the time to peak of EPSP ($p = 0.24$) or IPSP ($p = 0.66$) (Fig. 2.1F,G). These results indicate that the E/I balance in the FFI circuit of the TA pathway is abnormally increased in the *Fmr1* KO mice.

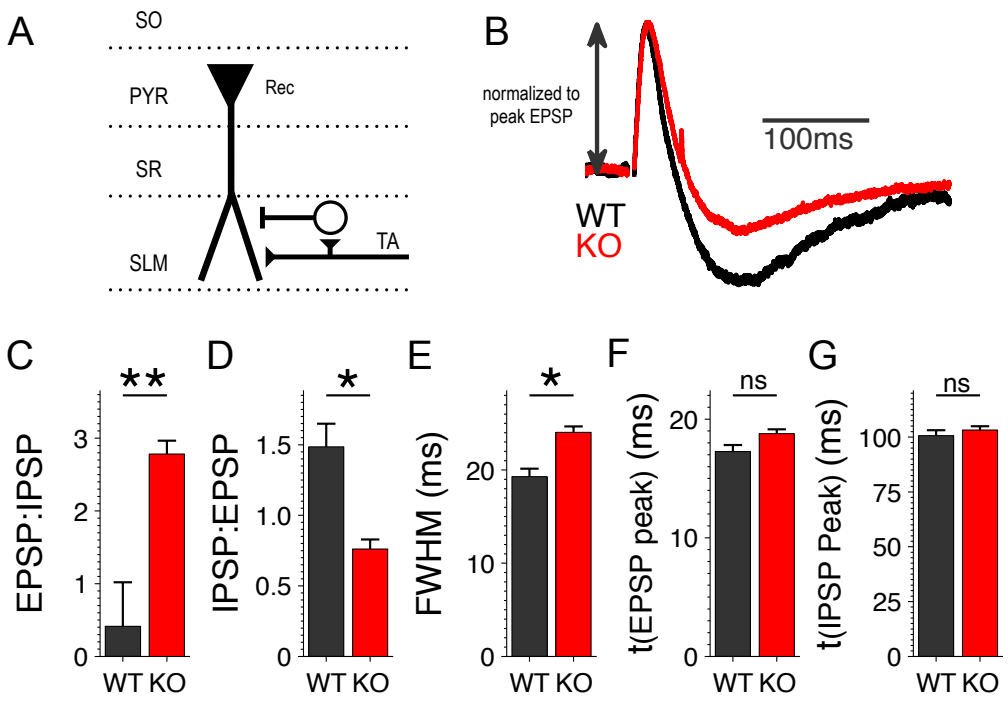

Figure 2.1 Abnormal E/I balance in the cortico-hippocampal feed-forward circuit of *Fmr1* KO mice

A. Schematic of stimulation protocol. Abbreviations denote hippocampal layers.

B. Average traces of the FFI circuit response to a single TA stimulus in WT (black) or *Fmr1* KO (red) mice. Traces are normalized to the peak of the excitatory response in each condition. n = 34(WT), 42(KO). Stimulus artifacts have been removed (here and throughout) for clarity.

C. Effect of FMRP loss on E/I ratio measured as a ratio of peak EPSP to peak IPSP in (B).

D. Effect of FMRP loss on I/E ratio measured as a ratio of peak IPSP to peak EPSP in (B).

E. Effect of FMRP loss on full-width at half-maximum (FWHM) of the EPSP in (B).

F, G. Effect of FMRP loss on the time to peak of EPSP (F) and IPSP (G) in (B).

**p<0.01, *p<0.05, ns – not significant.

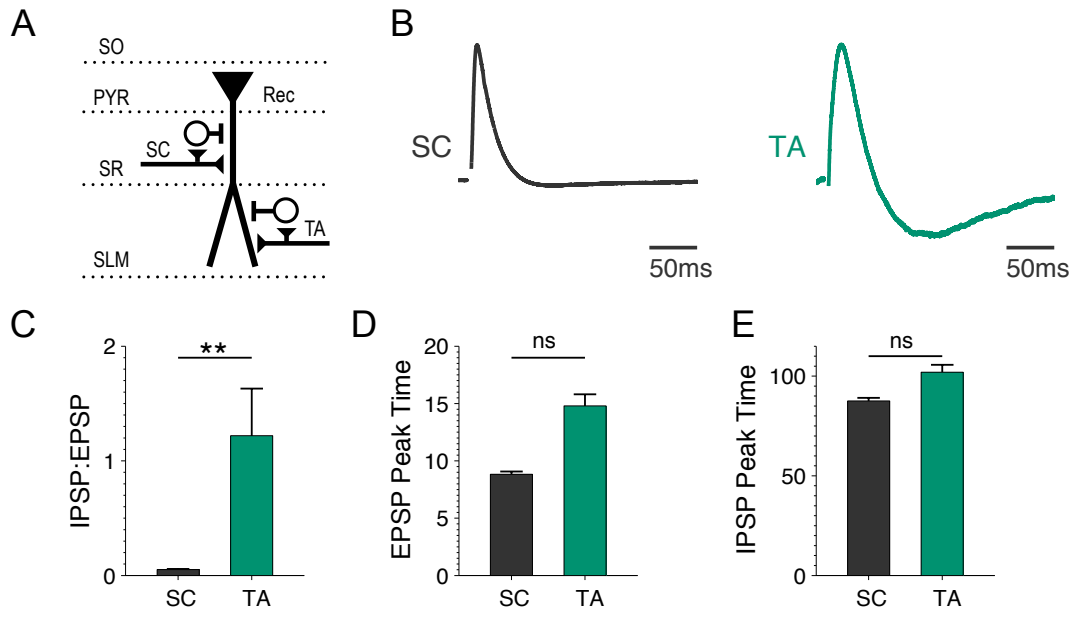

Figure 2.2 Differences in FFI circuit responses evoked by activation of the SC and TA pathways.

A. Schematic of stimulation protocol. Abbreviations denote hippocampal layers. FFI circuit responses to either SC or TA stimulus were recorded in the same CA1 neuron.

B. Average traces of the FFI circuit response to a single SC or TA stimulus. Traces are normalized to the peak of the excitatory response in each condition. Both responses are recorded in the same set of cells. $n = 6$.

C. Differences in pathway responses in I/E ratio measured as a ratio of peak IPSP to peak EPSP in (B).

D. Differences in pathway responses for the timing of peak of the EPSP in (B).

E. Differences in pathway responses for the timing of peak of the IPSP in (B).

2.3.2 Feed-forward inhibitory circuit dynamics are abnormal in Fmr1 KO mice

Next, we examined how the altered E/I balance affects the dynamics of feed-forward inhibition during high-frequency stimulus trains. Responses to three different stimulus frequencies—5Hz, 25Hz, and 40Hz—were examined (Fig. 2.3). Analysis of these data is complicated by the response waveform consisting of both excitatory and inhibitory components, each with independent dynamic changes throughout the train, and by the complex overlap of excitatory and inhibitory responses evoked by subsequent stimuli. Consequently, normalization to averaged baseline responses, which is typically used in such measurements to control for slice-to-slice stimulus variability (Klyachko and Stevens, 2006), is not applicable for these FFI measurements. To overcome this obstacle and still account for the stimulus intensity, we devised a different measure represented by the ratio of hyperpolarizing component (Yh) of the response to the depolarizing component of the response (Yd, relative to resting potential) following each stimulus (Fig. 2.3G). Analysis of FFI circuit responses recorded with and without the inhibitory component demonstrates that this measure robustly reflects the contribution of inhibition rather than the decay of EPSP (Fig. 2.4). This measure can be interpreted to represent a relative contribution of inhibition to the overall level of excitation in the FFI circuit during trains. We found that the Yh:Yd ratio was significantly reduced throughout the train in *Fmr1* KO relative to WT mice at two higher train frequencies (Fig. 2.3D-F; quantified in Fig. 3H; 5Hz: n = 7(WT), 8(KO), p = 0.95, 25Hz: n = 20(WT), 26(KO), p = 0.02; 40Hz: n = 16(WT), 19(KO), p = 0.03). These results indicate that the E/I balance and FFI circuit dynamics are abnormal during high-frequency trains in the TA pathway of *Fmr1* KO mice.

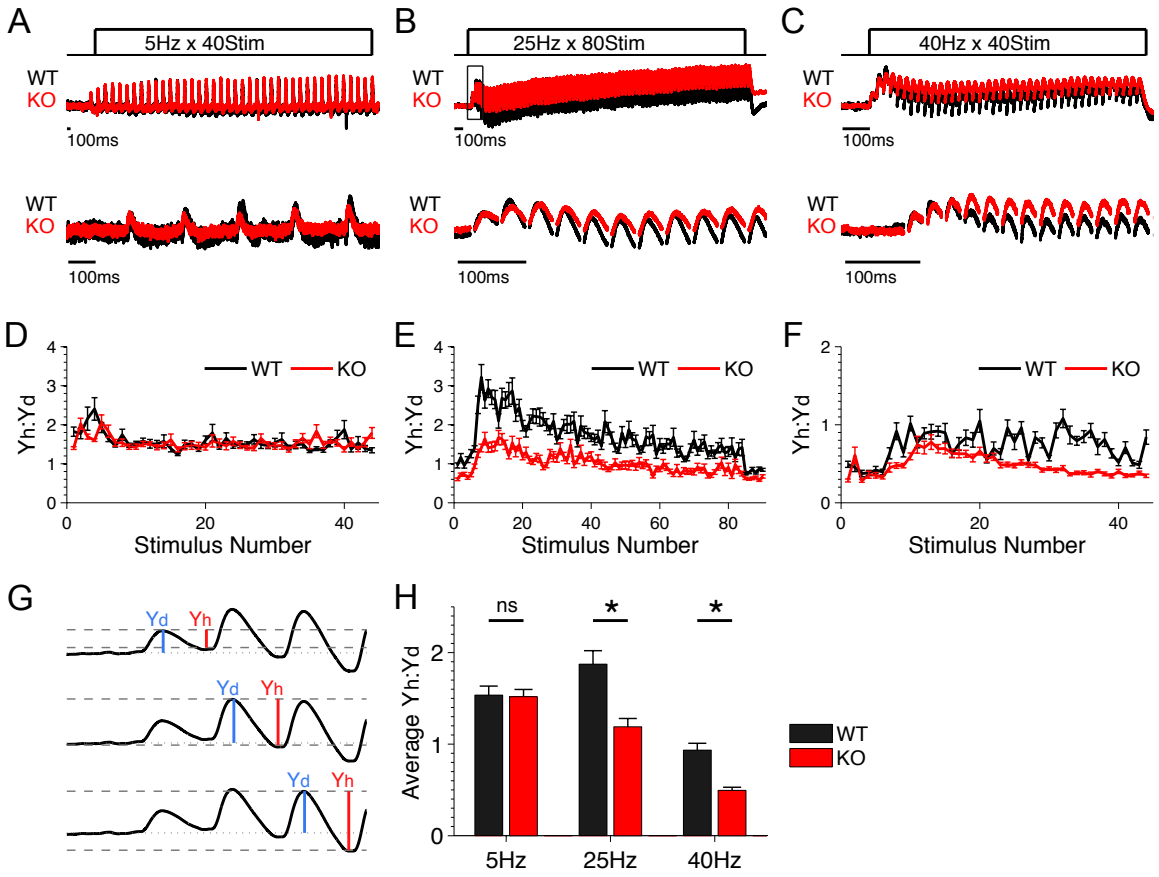

Figure 2.3 Abnormal E/I balance in the cortico-hippocampal feed-forward circuit of *Fmr1* KO mice during stimulus trains

A-C. Sample traces of FFI responses to 5Hz, 25Hz, and 40Hz, respectively. For visual comparison of dynamic changes during the trains, traces were normalized to the peak of the first response in the train, averaged across cells and then scaled to match the peak of the first response between WT and *Fmr1* KO. Boxed portion of 25Hz traces denotes areas enlarged in (G). Traces below show the representative examples of first several responses during trains in each condition.

D-F. Yh:Yd ratio was calculated for each stimulus in the 5Hz, 25Hz, and 40Hz trains, respectively. n = 7(WT 5Hz), 8(KO 5Hz), 20(WT 25Hz), 26(KO 25Hz), 24(WT 40Hz), 22(KO 40Hz).

G. Schematic of the Yh:Yd ratio analysis.

H. Summary of average Yh:Yd ratios during 5Hz, 25Hz and 40Hz trains.

**p<0.01, *p<0.05, ns – not significant.

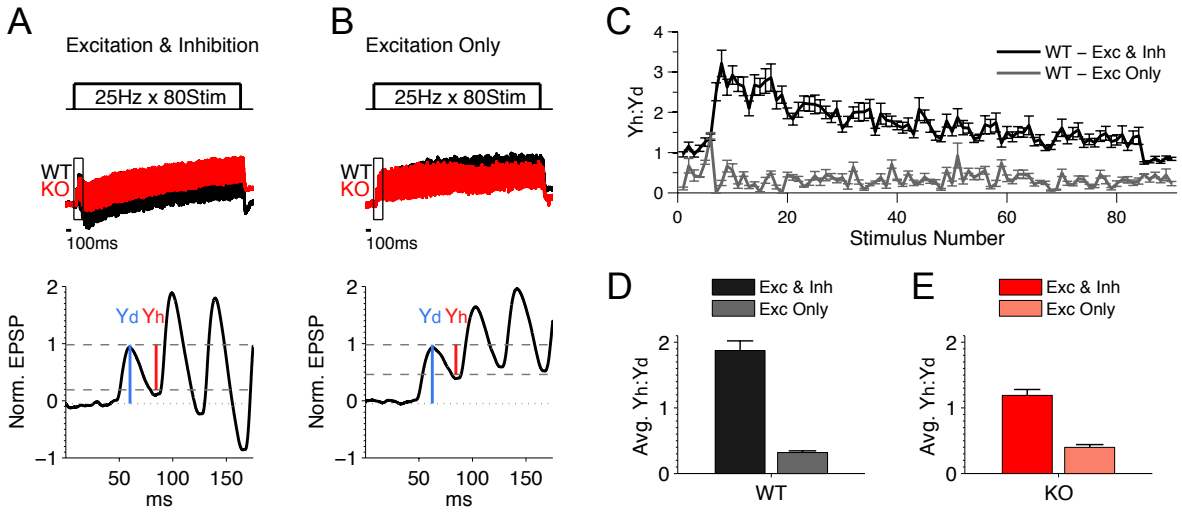

Figure 2.4 Yh:Yd ratio is a robust measure for the contribution of inhibition

A, B. Average traces of FFI responses to 25Hz stimulus, in WT and *Fmr1* KO mice, recorded with and without inhibition (+ Gabazine (5μM) and CGP55845 (2μM)) respectively. For visual comparison of dynamic changes during the trains, traces were normalized to the peak of the first response in the train, averaged across cells and then scaled to match the peak of the first response between WT and *Fmr1* KO. Boxed portion of 25Hz traces denotes areas enlarged in bottom traces for the KO trace. Schematic of the Yh:Yd ratios during 25Hz train for Excitation & Inhibition and Excitation Only, respectively are shown on the bottom panels. Panel A represents the same data as in Fig 2B**.** *n* = 20 (WT Excitation & Inhibition), 26 (KO Excitation & Inhibition), 7 (WT Excitation Only), 8 (KO Excitation Only).

C. Average Yh:Yd ratio for each stimulus in the 25Hz stimulus train with and without inhibition in WT.

D, E. Summary of average Yh:Yd ratios during 25Hz trains across all stimuli for WT and *Fmr1* KO mice. We note that Yh:Yd ratios represent predominately contribution of inhibition (excitation and inhibition) rather than the decay of EPSP (excitation only).

2.3.3 Defective spike modulation by the feed-forward circuits of Fmr1 KO mice

What are functional consequences of these abnormalities to the operations performed by FFI circuits? To approach this question, we used the spike modulation paradigm previously described by Remondes and Shuman, 2002, as it is known to be dependent on the FFI circuits. These studies have demonstrated that the converging inputs to the CA1 area of the hippocampus—the tri-synaptic pathway via Schaffer collaterals (SC) and the direct cortical input via the TA pathway—dynamically modulate each other via local FFI circuits. Single activation of the SC pathway, which alone is not capable of producing a spike in a postsynaptic neuron, has an enhanced ability to evoke a spike if it occurs coincidently with a train of stimuli in the TA pathway. Conversely, the ability of the SC pathway to evoke a spike is inhibited then SC activation follows the train of stimuli in the TA pathway within ~300ms. Both of these spike modulation functions depend on FFI circuits (Remondes and Schuman, 2002). Therefore, we tested whether these spike enhancing/blocking functions are affected in *Fmr1* KO mice. Spiking in the target CA1 neurons was recorded in a cell-attached mode while stimulating the SC pathway and the TA pathway with corresponding activity patterns (schematic in Fig. 2.5A). For the spike enhancement experiment, the SC pathway was stimulated with a single stimulus that alone was capable of producing a spike in the postsynaptic cell only 10% of the time, while the TA pathway was stimulated coincidently by a train of 10 stimuli at 100Hz (Fig. 2.5B). The probability of spike occurring was then measured at various time intervals (0 to 80ms) between the beginning of the stimulus train at the TA pathway and the single stimulus at the SC pathway (Fig. 2.5D). For the spike-blocking experiment, the SC pathway was stimulated at an intensity that evoked a postsynaptic spike 90% of the time (Fig. 2.5C). The probability that activation of

the TA pathway would block the occurrence of that spike was then measured at various time intervals following the TA pathway stimulus train (Fig. 2.5E). The *Fmr1* KO mice exhibited an increase in spike enhancement (Fig. 2.5D) and decease in spike blocking (Fig. 2.5E), consistent with the reduced FFI inhibition. The E/I imbalance thus has major implications to the spike modulation operations performed by the FFI circuits in *Fmr1* KO mice.

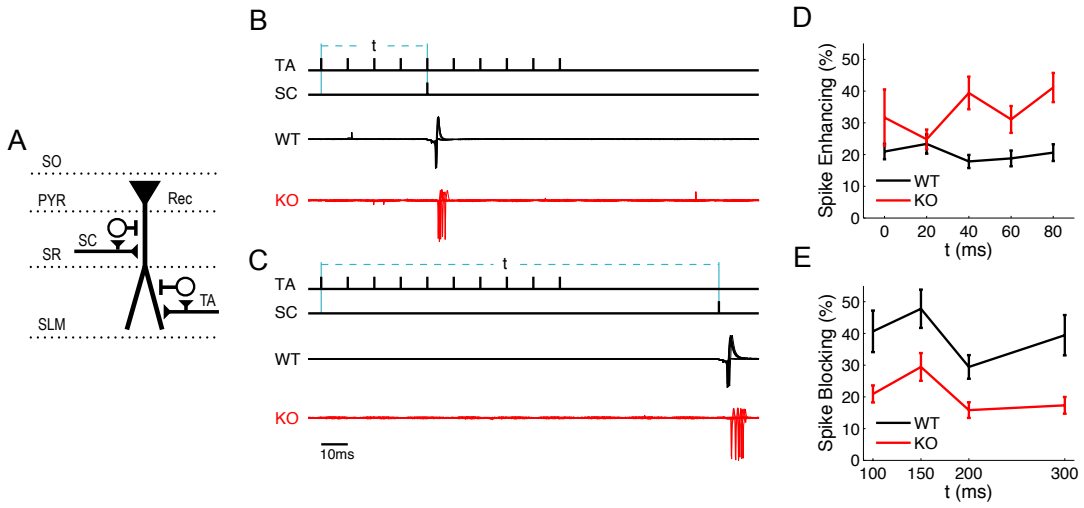

Figure 2.5 Abnormal spike modulation by the feed-forward circuits in *Fmr1* KO mice

A. Schematic of experimental set-up (SC - Schaffer collateral pathway, TA – Temporoammonic pathway).

B. Top: Schematic of a stimulation paradigm for heterosynaptic spike enhancement. The value t represents the time between the first TA pathway stimulus and the SC stimulus. Bottom: Overlay of 10 trails for a WT (black) and a *Fmr1* KO (red) neuron.

C. Same as (B) for spike blocking paradigm.

D. Spike enhancement as a function of time between the first stimulus of the TA pathway train (10 stimuli at 100Hz) and the single stimulus in SC pathway. $n = 4 – 9$ independent measurements per time point.

E. Same as (D) for spike blocking paradigm. t represents the time from the first stimulus of the TA pathway train to the stimulus in the SC pathway. Because the TA stimulus train is 90ms long, the first time point (t = 100) is at 10ms after the last TA pathway stimulation. $n = 4 – 9$ independent measurements per time point.

2.3.4 Excitatory synapse function is maintained in the TA pathway of Fmr1 KO mice

The observed abnormalities in E/I balance and FFI circuit properties could arise form changes in excitatory synapse function, inhibitory synapse function or both. To determine whether changes at the excitatory cortico-hippocampal TA pathway synapses were contributing to the FFI circuit defects, we pharmacologically isolated the excitatory component of the TA pathway input using Gabazine (5μM) and CGP55845 (2μM) to block $GABA_A$ and $GABA_B$ receptors, respectively. In the absence of inhibition, the EPSPs evoked in CA1 neurons by single TA pathway stimulation were indistinguishable in *Fmr1* KO and WT controls, both in terms of their width (Fig. 2.6A,B, WT: 24.0 ± 0.9ms, n = 7; KO: 21.2 ± 1.6ms, n = 6, p = 0.44) and timing of the peak (Fig. 2.6C, WT: 17.1 ± 0.8ms, KO: 18.6 ± 0.5ms, p = 0.44).

To further assess changes in excitatory synaptic transmission of the TA pathway input, we examined the short-term dynamics of the excitatory responses during high-frequency trains of 5-80Hz in voltage-clamped CA1 neurons of *Fmr1* KO and WT mice. For each stimulus frequency, we also calculated the paired-pulse ratio (PPR) by dividing the magnitude of the second EPSC of the train by the magnitude of the first EPSC of the train. We found no significant differences in the short-term dynamics of excitatory responses (Fig. 2.6E-G) or the PPR (Fig. 2.6D) between *Fmr1* KO and WT mice for any of the tested frequencies. Together these results indicate that the excitatory synaptic transmission at the TA pathway synapses is maintained in *Fmr1* KO mice. We note that this is in contrast to hippocampal CA3 and Layer 5 cortical excitatory neurons in which we previously found major presynaptic defects leading to abnormally elevated glutamate release during high-frequency trains (Deng et al., 2013; Deng et al., 2011; Myrick et al., 2015). This heterogeneity in synaptic defects caused by FMRP loss in different or even the same brain

areas is not surprising and has been documented in numerous previous studies of both excitatory and inhibitory synapses (Centonze et al., 2008; Curia et al., 2009; Olmos-Serrano et al., 2010; Patel et al., 2013; Patel et al., 2014; Wang et al., 2014a).

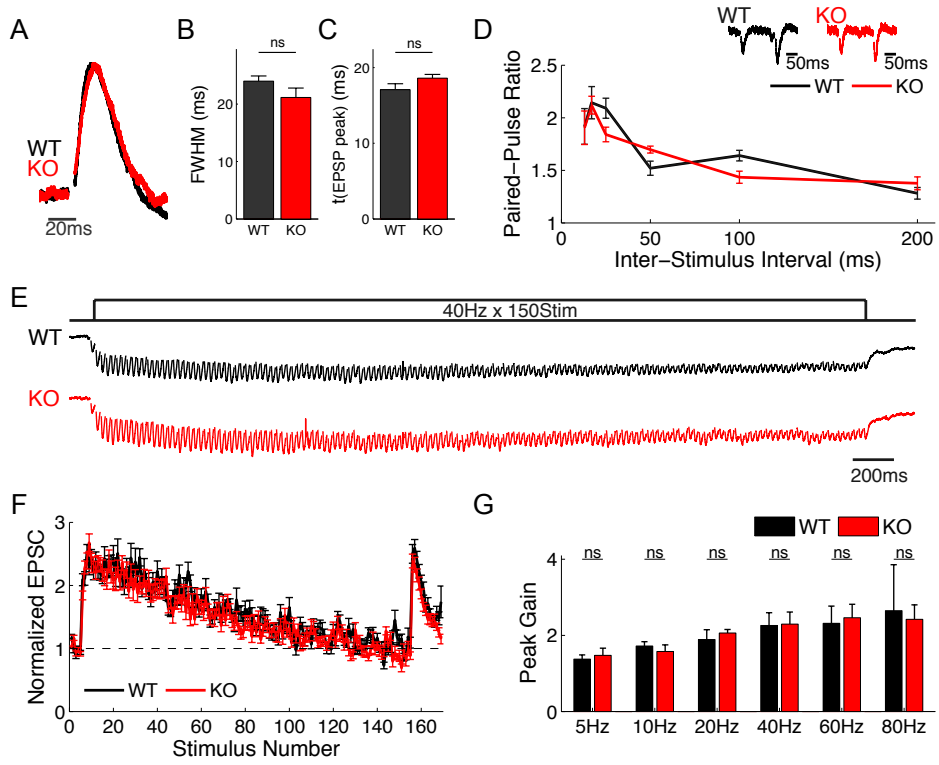

Figure 2.6. Excitatory synaptic transmission is normal in the TA pathway of *Fmr1* KO mice

A. Average trace of whole-cell EPSP evoked by a single stimulus in WT and *Fmr1* KO mice normalized to their peak values. n = 7(WT), 6(KO).

B. FWHM of average EPSP in (A).

C. Time to peak of EPSP in (A).

D. PPR measured at different time intervals. Sample traces shown on top. n = 8 -- 11 independent measurements per time point for each WT and *Fmr1* KO.

E. Traces of responses to 150 stimuli train at 40Hz recorded in voltage-clamp (V_{hold} = -60mV). Traces represent an average across cells and are low-pass median filtered for presentation only. n = 9(WT), 10(KO). We note that one WT cell was excluded from the average trace shown (for presentation only), because of a large recording artifact in the middle of the train.

F. Excitatory synaptic dynamics during 150 stimuli 40Hz trains recorded in voltage-clamp (shown in E). Peak EPSC values during the train were normalized to the averaged baseline EPSC preceding each train. n = 10(WT), 10(KO).

G. Maximal EPSC gain during the trains for various stimulus frequencies. n = 8 -- 11 independent measurements per frequency for each WT and *Fmr1* KO.

ns – not significant.

2.3.5 Altered GABA release in TA-associated inhibitory hippocampal synapses is mediated by $GABA_B$ receptor dysfunction in Fmr1 KO mice

The TA pathway fibers form excitatory synapses on CA1 pyramidal cells and also directly activate interneurons with the soma in the stratum lacunosum moleculare (SLM), which in turn project to CA1 pyramidal cells to form unitary FFI circuits (Empson and Heinemann, 1995b; Remondes and Schuman, 2002). The SLM layer of the hippocampus in the vicinity of the TA pathway contains the axons of many interneurons that participate in the TA feed-forward inhibition (Price et al., 2008). Therefore, we next examined properties of inhibitory synaptic inputs to the CA1 pyramidal neurons in the SLM layer. Excitation was blocked using APV (50μM) and DNQX (10μM) in the bath solution; the resulting IPSP evoked by a single TA pathway stimulus had a complex waveform that consisted of an early, predominately $GABA_A$ receptor ($GABA_AR$)-mediated potential followed by a late $GABA_B$ receptor ($GABA_BR$)-mediated potential (Empson and Heinemann, 1995a). To examine these components separately, we recorded IPSPs evoked by a single TA stimulus before and after adding a selective $GABA_BR$ antagonist CGP55845 (2μM) in the same cell. The data was then normalized to the peak of the early IPSP to account for variations in stimulus intensity between slices (for analysis of the late IPSP component see Fig. 9C,D and text below). Blocking $GABA_BRs$ caused an increase in the early IPSP (Fig. 7A), likely because this treatment alleviated the inhibitory influence of presynaptic $GABA_BRs$ on GABA release probability, in agreement with previous studies (Chalifoux and Carter, 2011). Most importantly, we observed that the IPSP increase in the presence of $GABA_BR$ antagonist was significantly larger in *Fmr1* KO than in the WT mice (Fig. 2.7B, WT: 1.24 ± 0.03, $n = 9$; KO: 1.50 ± 0.02 $n = 6$, $p = 0.04$) suggesting an excessive $GABA_B$-R signaling in these inhibitory synapses of *Fmr1* KO mice. We note that although $GABA_BR$ antagonist inhibits both pre- and postsynaptic $GABA_BRs$, blocking postsynaptic $GABA_BRs$

cannot increase an early IPSP in these recordings. These results suggest that $GABA_BR$-mediated inhibition of GABA release is abnormally elevated in *Fmr1* KO mice.

To further examine changes in GABA release probability, we used PPR measurements. We found a shift from paired-pulse depression to facilitation in *Fmr1* KO compared to WT mice (Fig. 2.7C, WT: 0.83 ± 0.05, n =17; KO: 2.11 ± 0.43, n = 13; p = 0.04), consistent with reduced GABA release probability (Deng and Klyachko, 2011). This difference in the PPR between *Fmr1* KO and WT mice was eliminated by $GABA_BR$ antagonist CGP55845 (Fig. 2.7C, WT: 0.91 ± 0.05, n = 9; KO: 1.22 ± 0.15, n = 6; p = 0.45), further supporting the role of presynaptic $GABA_BRs$ in this defect.

To further examine the origins of the above GABAergic transmission defects, we measured the coefficient of variation (CV) of IPSPs, which has been previously shown to represent a measure specifically of presynaptic function (Fitzjohn et al., 2001; Kullmann, 1994; Wang et al., 2014b). CV of the early IPSP component was significantly increased in *Fmr1* KO relative to WT mice (Fig. 2.7D, WT: 0.20 ± 0.02, n = 9; KO: 0.37 ± 0.04, n = 6; p = 0.03), consistent with the presynaptic origin of the IPSP changes. These differences in CV were eliminated by the application of the $GABA_BR$ antagonist in the same cells (Fig. 2.7D, WT: 0.19 ± 0.01, n = 9; KO: 0.23 ± 0.02, n = 6; p = 0.68), supporting the role of presynaptic $GABA_BRs$ in these changes.

We sought to corroborate these findings by examining the short-term dynamics of the inhibitory synapses during trains of stimuli (80 stimuli at 25Hz) without and with the $GABA_BR$ antagonist. As expected from the above results, the short-term dynamics in the *Fmr1* KO mice deviated qualitatively from that in WT mice with a strongly increased facilitation at the beginning of the train (Fig. 2.7E). As in the above experiments, these differences were also eliminated by the $GABA_BR$ antagonist (Fig. 2.7E).

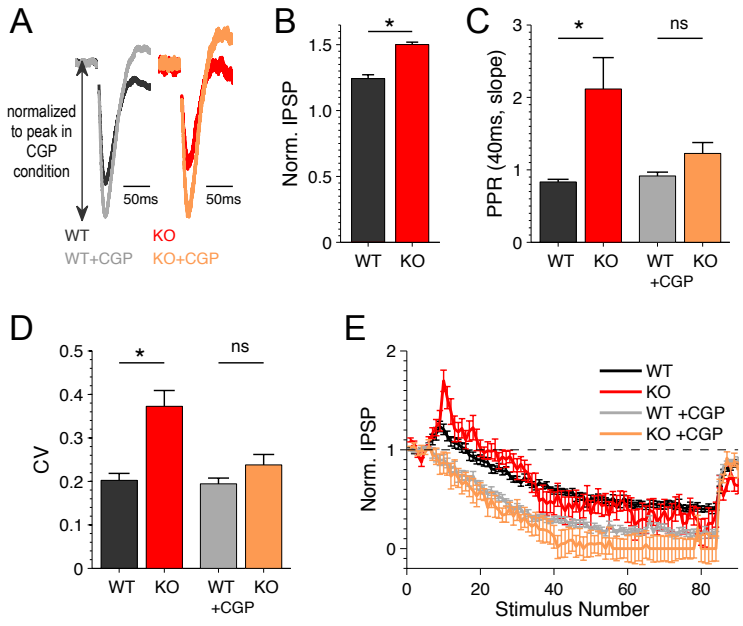

Figure 2.7. Dysfunction of TA-associated inhibitory synapses in *Fmr1* KO mice is $GABA_B$ receptor dependent.

A. Average IPSP evoked by a single TA stimulation before and after bath application of $GABA_BR$ antagonist CGP55845 (2μM). Excitation was blocked with CNQX (10 μM) and APV (50μM) in all experiments shown in A-E. *n* = 9(WT), 6(KO). CGP – CGP55845 (here and below).

B. Ratio of average IPSP magnitude recorded after/before application of CGP55845. *n* = 9(WT), 6(KO).

C. PPR determined at 40ms interval based on IPSP slopes in the presence (*n* = 9(WT), 6(KO)) /absence(*n* = 17(WT), 13(KO)) of CGP55845.

D. CV determined in the presence/absence of CGP55845. *n* = 9(WT), 6(KO).

E. Average inhibitory responses during 25Hz trains, in the absence (*n* = 17(WT), 13(KO))/presence(*n* = 9(WT), 6(KO)) of CGP55845) normalized to an average baseline response for each condition.

*p<0.05, ns – not significant

We further examined whether these $GABA_BR$-mediated abnormalities are specific to the inhibitory synapses in the SLM layer, or if similar abnormalities are also present in inhibitory synapses in the stratum radiatum (SR) that contains the axons of many interneurons that participate in feed-forward inhibition of the SC pathway. Inhibitory synaptic transmission was evoked in the CA1 neurons by SR stimulation in the presence of APV (50μM) and DNQX (10μM) in the bath solution. In contrast with the SLM stimulation described above, we observed no significant differences between *Fmr1* KO and WT animals in any of the measurements of presynaptic function (Fig 2.8B-D), in agreement with our earlier studies (Deng et al., 2011). Moreover, we did not observe measurable effects of $GABA_BR$ antagonist in either WT or *Fmr1* KO animals in any of presynaptic measurements performed (Fig. 2.8B-D), indicating that the inhibitory synapses in the SR do not contain significant presynaptic $GABA_BR$ –mediated activity.

Taken together these results suggest that GABA release at inhibitory SLM synapses on CA1 neurons is reduced in *Fmr1* KO mice in a selective manner. Our results are consistent with the major role of presynaptic $GABA_BRs$ in this defect, which we investigate further below.

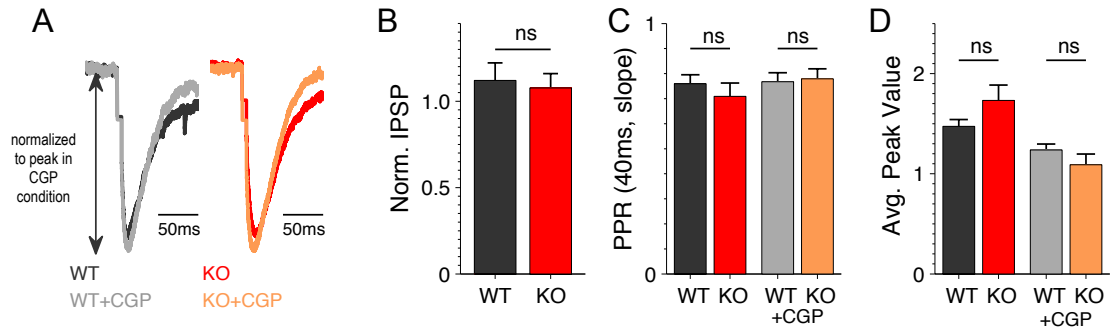

Figure 2.8. SC-associated inhibitory hippocampal synapses in stratum radiatum do not exhibit presynaptic or $GABA_BR$-dependent abnormalities in *Fmr1* KO mice.

A. Average IPSP evoked in CA1 pyramidal neurons by a single stimulation in SR before and after bath application of $GABA_BR$ antagonist CGP55845 (2μM). Recordings were performed at -45mV. Excitation was blocked with CNQX (10 μM) and APV (50μM) in all experiments shown in A-D. *n* = 6(WT), 6(KO). CGP – CGP55845 (here and below).

B. Ratio of average IPSP magnitude recorded after/before application of CGP55845. *n* = 6(WT), 6(KO).

C. PPR was determined at 40ms interval based on IPSP slopes in the presence/absence of CGP55845. *n* = 6(WT), 6(KO).

D. Analysis of short-term dynamics during 25Hz, 80 stimuli trains. Peak values during the train were determined as an average of responses 10 to 15 (around the point where the train responses reach maximum value). n = 6(WT), 6(KO).

ns – not significant

2.3.6 Presynaptic GABAB-receptor dysfunction plays a major role in abnormal feed-forward inhibition in the TA pathway of Fmr1 KO mice

The above results point to $GABA_BR$ signaling defects as a major cause of abnormal inhibitory synapse function in the TA pathway of *Fmr1* KO mice. SLM inhibitory fibers activated by TA pathway stimulation in the above experiments may not, however, fully represent the population of interneurons involved in FFI. Therefore, we examined the role of $GABA_BR$ signaling in the abnormalities of the intact FFI circuit of the TA pathway. The FFI circuit activity was evoked and recorded as described above (Fig. 2.1) using both single stimuli and high-frequency trains. We found that differences between *Fmr1* KO and WT mice were no longer significant in the presence of $GABA_BR$ antagonist for both the I/E ratio measured for a single stimulus (Fig. 2.9A, n = 7(WT), 5(KO), p = 0.26) and for the average Yh:Yd ratio during the trains (Fig. 2.9B, n = 9(WT), 6(KO), p = 0.61).

Additionally, we examined the changes in the late component of inhibition by quantifying the inhibition levels at the peak of the late component (150ms after the stimulus), both with and without the $GABA_BR$ antagonist. Similarly to the early component of inhibition examined above, we found significant differences in the E/I ratio for the late component of inhibition between *Fmr1* KO and WT mice evoked by a single TA stimulation (Fig. 2.9C, p = 0.01). As in the above experiments, these differences were minimized by the addition of the $GABA_BR$ antagonist (Fig. 2.9C, p = 0.053). In this case, there were no *Fmr1* KO neurons that had measurable amounts of the late component of inhibition remaining after the addition of the $GABA_BR$ antagonist. Similar results were obtained for the late component of inhibition following the last stimulus of the train, which was significantly different between *Fmr1* KO and

WT mice (Fig. 2.9D, p = 0.04), and these differences were also eliminated by the $GABA_BR$ antagonist (Fig. 2.9D, p = 0.69).

Together, these results indicate that $GABA_BR$ signaling defects is a major cause of abnormal E/I balance in the intact FFI circuit of *Fmr1* KO mice.

Because the early component of inhibition is mediated predominately by $GABA_ARs$, the $GABA_BR$-dependent changes in this early component of inhibition in *Fmr1* KO mice reflect the role of presynaptic $GABA_BRs$ in controlling GABA release, but not the changes in postsynaptic $GABA_BRs$ properties. Changes in the late component of inhibition, on the other hand, could arise either from altered GABA release onto normal postsynaptic $GABA_BRs$, from altered postsynaptic $GABA_BR$ properties, or both. $GABA_BR$ subunits are differentially expressed at pre- and postsynaptic compartments (Guetg et al., 2009; Perez-Garci et al., 2006). Although no antagonists specifically targeting pre- or postsynaptic $GABA_BRs$ have been described thus far, earlier studies have shown that low concentrations (<1μM) of baclofen preferentially activate the pre-synaptic $GABA_BRs$ (Cruz et al., 2004; Guetg et al., 2009). Therefore, to determine if the E/I imbalance phenotype observed in *Fmr1* KO mice could be reproduced in the WT FFI circuit by selective activation of the presynaptic $GABA_BRs$, we used low concentrations of baclofen (0.5μM) applied to the bath. I/E circuit measurements were performed as described above. We found that application of low concentrations of baclofen in WT mice fully mimicked the abnormalities in I/E ratio evoked by a single stimulus in *Fmr1* KO mice both for early and late components of inhibition (Fig. 2.9A,C; I/E ratio measured at peak; WT+baclofen: 0.68 ± 0.11, n = 9; KO: 0.76 ± 0.05, n = 42, p = 0.99; I/E ratio for the late component of inhibition measured 150ms after the stimulus: WT+baclofen: 0.35 ± 0.07, n = 9; KO: 0.50 ± 0.05, n = 42, p = 0.45).

Additionally, application of low concentrations of baclofen in WT mice eliminated differences with *Fmr1* KO mice in average Yh:Yd ratio during the trains (Fig. 2.9B, WT+baclofen: 0.61±0.04, n = 12; KO: 0.50 ± 0.03 n = 22, p = 0.15), and in the late component of inhibition measured 150ms after the end of the train (Fig. 2.9D, WT+baclofen: 0.04 ± 0.01, n = 12; KO: 0.09 ± 0.01 n = 22, p = 0.37). Therefore, our results show that either blocking all $GABA_BRs$ or preferentially activating presynaptic $GABA_BRs$ in WT neurons largely eliminate differences in E/I circuit imbalance in the intact FFI circuit between *Fmr1* KO and WT mice. Taken together, these results indicate that $GABA_BR$ abnormalities play a critical role in FFI circuit dysfunction in the TA pathway of *Fmr1* KO mice, with a major contribution from presynaptic $GABA_BR$ defects.

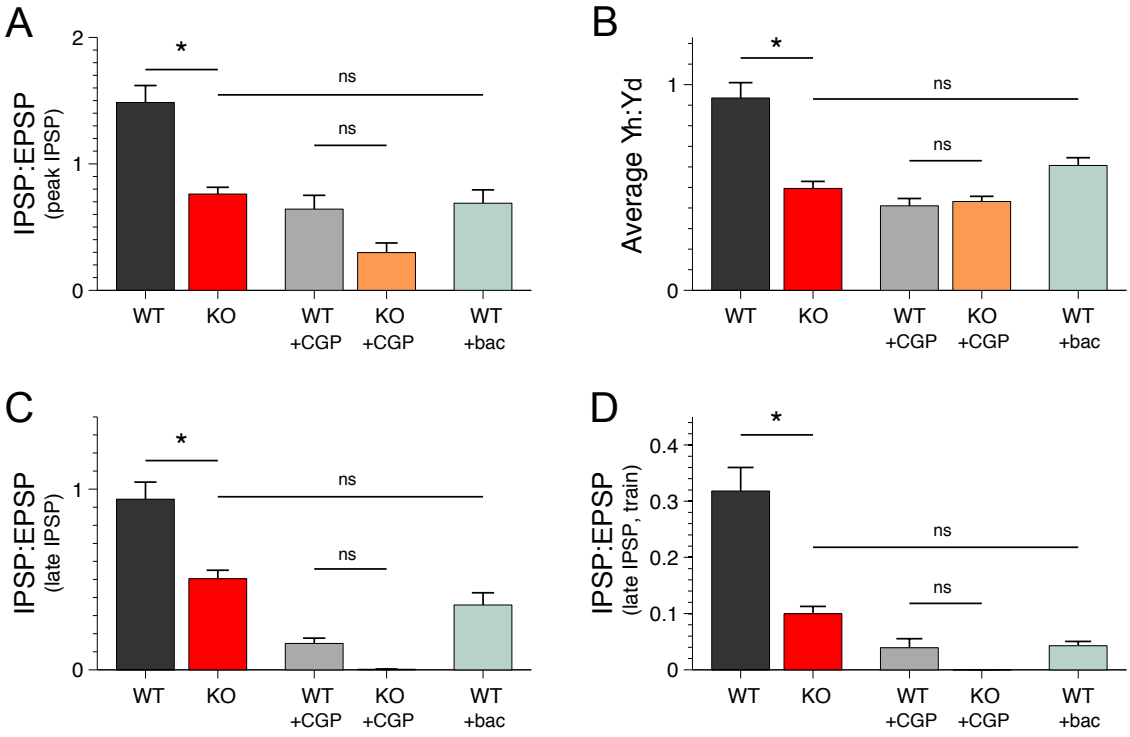

Figure 2.9. E/I imbalance in the FFI circuit of *Fmr1* KO mice is $GABA_B$ receptor dependent.

A. Ratio of IPSP to EPSP (inhibition measured at peak) for a baseline response evoked by a single stimulus in the intact FFI circuit of the TA pathway under specified conditions. (CGP – CGP55845, bac – baclofen). *n* = 34(WT), 42(KO), 7(WT+CGP), 5(KO+CGP), 9(WT+bac).

B. Average Yh:Yd ratio measured in the intact FFI circuit during a 40 stimuli 40Hz train under specified conditions. *n* = 24(WT), 22(KO), 9(WT+CGP), 6(KO+CGP), 12(WT+bac).

C. Ratio of IPSP to EPSP for the late component of inhibition (measured 150ms after the stimulus) for a baseline response evoked by a single stimulus in the intact FFI circuit of the TA pathway under specified conditions. *n* = 34(WT), 42(KO), 7(WT+CGP), 5(KO+CGP), 9(WT+bac).

D. Ratio of IPSP to EPSP for the late component of inhibition (measured 150ms after the stimulus) determined in the intact FFI circuit following the last stimulus in the 40 stimuli, 40Hz train under specified conditions. *n* = 24(WT), 22(KO), 9(WT+CGP), 6(KO+CGP), 12(WT+bac).

*$p<0.05$, ns – not significant

2.4 Discussion

While the dysfunction of the GABAergic system is well documented in FXS models, the underlying mechanisms and implications to circuit operations remain to be elucidated (Braat and Kooy, 2014). In the present study, we identified a major defect in the properties and function of a canonical FFI circuit formed by the cortico-hippocampal TA pathway in *Fmr1* KO mice. The observed marked E/I imbalance in the FFI circuit resulted specifically from reduced TA inhibition in the *Fmr1* KO mice, while the excitatory component of this circuit remained unaffected by FMRP loss. $GABA_A$-Rs and $GABA_B$-Rs mediate two main components of the GABAergic synaptic transmission, the early and late respectively. Several studies have implicated inhibitory synapse defects in the circuit hyperexcitability in FXS, but thus far, inhibitory synapse dysfunction has been largely attributed to the $GABA_A$-R-mediated abnormalities (Centonze et al., 2008; Curia et al., 2009; D'Hulst et al., 2006; Gantois et al., 2006; Martin et al., 2014; Olmos-Serrano et al., 2010; Paluszkiewicz et al., 2011). While $GABA_A$-Rs support rapid GABAergic synaptic transmission, $GABA_B$-Rs are metabotropic G protein-coupled receptors that are found both pre- and postsynaptically throughout the brain, where they provide powerful modulatory control of many aspects of synaptic function (Chalifoux and Carter, 2011). Whether $GABA_B$-R signaling is also affected by FMRP loss and whether it contributes to circuit deficits in FXS remains largely unexplored.

Our results suggest that the E/I imbalance and abnormal FFI circuit properties in the TA pathway of *Fmr1* KO mice are mediated by a $GABA_B$-R dysfunction, with a major contribution from presynaptic $GABA_B$-R-dependent reduction in GABA release. This model is supported by four lines of evidence. First, in inhibitory TA-associated synapses, the early, $GABA_A$R-

mediated component of IPSP is more sensitive to inhibition of $GABA_B$-Rs in *Fmr1* KO mice, suggesting excessive $GABA_B$-R activation or downstream signaling. While $GABA_B$-R antagonist inhibits both pre- and postsynaptic receptors, the increase in early IPSP produced by the antagonist cannot be caused by inhibition of postsynaptic $GABA_B$-Rs, which can only have an opposite effect on IPSP amplitude. Second, TA-associated inhibitory synapses in *Fmr1* KO mice have altered PPR, CV, and short-term dynamics which are all widely believed to reflect changes in presynaptic release probability (Fitzjohn et al., 2001; Kullmann, 1994; Rotman et al, 2011; Wang et al., 2014b), and these defects are also corrected by inhibition of $GABA_B$-Rs. Third, differences between *Fmr1* KO and WT mice in the E/I balance measured in the intact FFI circuit were eliminated by $GABA_B$-Rs inhibition or by preferential activation of presynaptic $GABA_B$-Rs with low concentrations of baclofen in WT mice. The mimicking effect of low baclofen concentrations in WT mice suggests that when the post-synaptic components are largely unaltered, a selective change in GABA release probability could account for the major defects in the E/I circuit balance in the TA pathway of *Fmr1* KO mice. Finally, the observation that preferential activation of presynaptic $GABA_B$-Rs eliminated differences between *Fmr1* KO and WT mice in the late component of inhibition, suggests that the postsynaptic $GABA_B$-Rs are not strongly affected in this circuit in *Fmr1* KO mice. The similar and seemingly contradictory effects of $GABA_B$-Rs agonist and antagonist may be understood by considering that $GABA_B$-R antagonist has a dual effect, acting on both pre- and postsynaptic receptors. Consequently, it relieves presynaptic $GABA_B$-R-dependent inhibition of GABA release thereby eliminating the differences between *Fmr1* KO and WT mice, but also acting postsynaptically to reduce GABA-evoked inhibition in postsynaptic neurons. Hence, the overall effect of the $GABA_B$-R antagonist is reduction in FFI inhibition in WT and *Fmr1* KOs to the same levels. Preferential activation of

presynaptic $GABA_B$-Rs with low concentrations of baclofen also reduces FFI levels, but does so by preferentially inhibiting presynaptic GABA release without strongly affecting the postsynaptic receptors. Altogether, these results support the major role of abnormal presynaptic $GABA_B$-R signaling in reduced GABA release and E/I imbalance in the TA pathway *of Fmr1* KO mice.

Our results do not exclude other mechanisms besides altered presynaptic $GABA_B$-R properties that may contribute to the inhibitory synapse defects in *Fmr1* KO mice. $GABA_B$-Rs act via G-protein activation on a large number of different downstream targets including voltage-dependent K^+ and Ca^{2+} channels, adenylate cyclase as well as components of the exocytotic release machinery (Chalifoux and Carter, 2011). $GABA_B$-Rs are also modulated by the auxiliary binding proteins, such as GISP, mupp1 and KCTD, which regulate $GABA_B$-R surface expression and function (Chalifoux and Carter, 2011). Elucidating whether abnormalities in the $GABA_B$-R protein levels, surface expression, auxiliary binding proteins or the downstream signaling pathways mediate the inhibitory synapse defects and E/I circuit imbalance in *Fmr1* KO mice will require a separate investigation. Additionally, over 20 different types of inhibitory interneurons have been identified (Lovett-Barron and Losonczy, 2014), and it remains unknown which subset of interneuron types are involved in FFI circuits. Recent study has identified neurogliaform cells as a major contributor to FFI circuit in the TA pathway, and revealed that GABA release in these cells is strongly modulated by presynaptic $GABA_B$-Rs (Price et al., 2008). While our observations are consistent with the role of neurogliaform cells in the FFI defects in *Fmr1* KO mice, elucidating whether this and/or other interneuron types mediate the FFI defects in FXS circuits will require extensive additional knowledge about interneuron functional specificity, which is not currently available.

$GABA_B$-Rs have attracted extensive recent attention as a potential target to correct hyperactivation of glutamatergic pathways and normalize behavioral phenotypes in *Fmr1* KO mice and FXS patients. A $GABA_B$-R agonist, arbaclofen, has been shown to correct multiple phenotypes in glutamatergic neurons of *Fmr1* KO mice (Berry-Kravis et al., 2012; Henderson et al., 2012; Pacey et al., 2011). However, arbaclofen treatment did not result in significant improvements in patients and its clinical trials have been discontinued. This treatment approach is based on the assumption that $GABA_B$-R agonists act predominately at excitatory nerve terminals to reduce glutamate release and dampen circuit excitability. Our results, however, suggest that $GABA_B$-Rs play a much more complex role in FXS, in which excessive presynaptic $GABA_B$-R signaling occurs in the inhibitory synapses where these receptors act to suppress GABA release and consequently promote circuit hyperexcitability in *Fmr1* KO mice. Application of $GABA_B$-R agonists will further reduce GABA release and promote circuit hyperexcitability, consequently, opposing the effect of the same compound at excitatory synapses. Indeed, $GABA_B$-Rs are located presynaptically on both excitatory and inhibitory synaptic terminals, as well as postsynaptically in the dendrites of both excitatory and inhibitory neurons thereby having complex and often opposing roles in modulating circuit excitability (Chalifoux and Carter, 2011). The difficulties in employing $GABA_B$-R signaling to regulate circuit excitability are further suggested by the heterogeneity of receptor expression in a cell-type and domain-specific manner (Ault and Nadler, 1982; Laviv et al., 2010; Price et al., 2008). Based on these considerations, $GABA_B$-R agonists are expected to affect both GABA and glutamate release and thereby have complex, rather than unidirectional, effects on circuit excitability, which are also likely to be cell-type and circuit-specific.

An additional complexity in directly applying synaptic-level findings to the treatment of FXS will likely arise from the heterogeneity of excitatory and inhibitory synaptic defects observed in different circuits and brain regions (Centonze et al., 2008; Curia et al., 2009; Gibson et al., 2008; Olmos-Serrano et al., 2010; Patel et al., 2013; Wang et al., 2014a). For instance, we have previously described a major presynaptic defect in the excitatory hippocampal CA3 and Layer 5 cortical pyramidal neurons associated with excessive AP broadening and excessive glutamate release (Deng et al., 2013). In contrast, here we found that glutamate release is unaffected in TA pathway excitatory synapses of *Fmr1* KO mice formed onto the same population of CA1 neurons by the Layer 3 cortical inputs. Furthermore, we observed a complementary set of changes in inhibitory hippocampal synapses, with defects evident in the TA- but not in SC-associated inhibitory synapses onto CA1 pyramidal neurons. This heterogeneity is not surprising, however, and has been described in many previously studies. For example, cortical excitatory synapses onto inhibitory fast-spiking interneurons exhibit marked presynaptic defects in *Fmr1* KO mice while excitatory synapses of the same neuron on different targets are normal (Patel et al., 2013). Similarly, large heterogeneity has been reported for the extent and direction of GABAergic transmission defects in *Fmr1* KO mice (Centonze et al., 2008; Curia et al., 2009; Gibson et al., 2008; Olmos-Serrano et al., 2010). $GABA_B$-R defects are also likely to be circuit and cell-type specific, since a high degree of heterogeneity in $GABA_B$-R signaling is present even for excitatory synapses converging onto the same population of hippocampal neurons (Laviv et al., 2010). Specifically, in the hippocampus, excitatory cortical inputs of the TA pathway onto CA1 pyramidal neurons do not contain measurable levels of presynaptic $GABA_B$-Rs, while the excitatory SC synapses onto the same population of CA1 neurons do (Laviv et al., 2010). We found here that the opposite is the case for the TA- and SC-pathway-associated inhibitory

hippocampal synapses. Our current findings suggest that extensive additional investigation is needed to better understand the complexity and diversity of $GABA_B$-R signaling and its role in FXS neuropathology.

How does E/I imbalance in the basic FFI circuit we observed here contribute to FXS neuropathology? FFI circuits play key roles in many information-processing operations (Chittajallu et al., 2013; Dudman et al., 2007; Ferrante et al., 2009; Gabernet et al., 2005; Han and Heinemann, 2013; Izumi and Zorumski, 2008; Klyachko and Stevens, 2006). In particular, the FFI circuits of the TA pathway are known to be involved in the induction and tuning of multiple forms of heterosynaptic plasticity at the Schaffer collateral synapses (Dudman et al., 2007; Han and Heinemann, 2013; Izumi and Zorumski, 2008), for the generation and maintenance of the theta frequencies (Ang et al., 2005), as well as for overall hippocampal information flow (Basu et al., 2013). Alterations in the FFI properties have many critical implications for the local network functionality. Indeed, we found that the altered E/I ratio has major implications to the fundamental operations performed by the FFI circuits in *Fmr1* KO mice. Specifically, the coincidence detection-based modulation of spiking probability in the target excitatory neuron was abnormally shifted in *Fmr1* KO mice towards excessive enhancement of spiking at short time intervals and reduced spike blocking at longer intervals. This hyperactive spiking behavior implies a reduction in ability to discriminate the incoming spike patterns. The FFI circuit function is therefore abnormally shifted in a way that blunts its ability for coincidence detection and further promotes circuit hyperexcitability. Given that precise E\I balance is required for proper FFI circuit functioning (Chittajallu et al., 2013; Ferrante et al., 2009; Gabernet et al., 2005; Pouille and Scanziani, 2001; Remondes and Schuman, 2002), we predict that many other FFI circuit operations are likely to be abnormal in

the FXS mouse model. Our results provide a first step towards further investigation into local circuit dysfunction in FXS and the role of $GABA_BR$ signaling in these defects.

References

Ang, C.W., Carlson, G.C., and Coulter, D.A. (2005). Hippocampal CA1 circuitry dynamically gates direct cortical inputs preferentially at theta frequencies. J Neurosci *25*, 9567-9580.

Ault, B., and Nadler, J.V. (1982). Baclofen selectively inhibits transmission at synapses made by axons of CA3 pyramidal cells in the hippocampal slice. J Pharmacol Exp Ther *223*, 291-297.

Bassell, G.J., and Warren, S.T. (2008). Fragile X syndrome: loss of local mRNA regulation alters synaptic development and function. Neuron *60*, 201-214.

Basu, J., Srinivas, K.V., Cheung, S.K., Taniguchi, H., Huang, Z.J., and Siegelbaum, S.A. (2013). A cortico-hippocampal learning rule shapes inhibitory microcircuit activity to enhance hippocampal information flow. Neuron *79*, 1208-1221.

Berry-Kravis, E.M., Hessl, D., Rathmell, B., Zarevics, P., Cherubini, M., Walton-Bowen, K., Mu, Y., Nguyen, D.V., Gonzalez-Heydrich, J., Wang, P.P.*, et al.* (2012). Effects of STX209 (arbaclofen) on neurobehavioral function in children and adults with fragile X syndrome: a randomized, controlled, phase 2 trial. Sci Transl Med *4*, 152ra127.

Braat, S., and Kooy, R.F. (2014). Insights into GABAergic system deficits in fragile X syndrome lead to clinical trials. Neuropharmacology. 88C:48-54.

Centonze, D., Rossi, S., Mercaldo, V., Napoli, I., Ciotti, M.T., De Chiara, V., Musella, A., Prosperetti, C., Calabresi, P., Bernardi, G., and Bagni, C. (2008). Abnormal striatal GABA transmission in the mouse model for the fragile X syndrome. Biol Psychiatry *63*, 963-973.

Chalifoux, J.R., and Carter, A.G. (2011). GABAB receptor modulation of synaptic function. Curr Opin Neurobiol *21*, 339-344.

Chittajallu, R., Pelkey, K.A., and McBain, C.J. (2013). Neurogliaform cells dynamically regulate somatosensory integration via synapse-specific modulation. Nat Neurosci *16*, 13-15.

Cruz, H.G., Ivanova, T., Lunn, M.L., Stoffel, M., Slesinger, P.A., and Luscher, C. (2004). Bi-directional effects of GABA(B) receptor agonists on the mesolimbic dopamine system. Nat Neurosci *7*, 153-159.

Curia, G., Papouin, T., Seguela, P., and Avoli, M. (2009). Downregulation of tonic GABAergic inhibition in a mouse model of fragile X syndrome. Cerebral cortex *19*, 1515-1520.

D'Hulst, C., De Geest, N., Reeve, S.P., Van Dam, D., De Deyn, P.P., Hassan, B.A., and Kooy, R.F. (2006). Decreased expression of the GABAA receptor in fragile X syndrome. Brain Res *1121*, 238-245.

Deng, P.Y., and Klyachko, V.A. (2011). The diverse functions of short-term plasticity components in synaptic computations. Commun Integr Biol *4*, 543-548.

Deng, P.Y., Rotman, Z., Blundon, J.A., Cho, Y., Cui, J., Cavalli, V., Zakharenko, S.S., and Klyachko, V.A. (2013). FMRP regulates neurotransmitter release and synaptic information transmission by modulating action potential duration via BK channels. Neuron *77*, 696-711.

Deng, P.Y., Sojka, D., and Klyachko, V.A. (2011). Abnormal presynaptic short-term plasticity and information processing in a mouse model of fragile x syndrome. J Neurosci *31*, 10971-10982.

Dudman, J.T., Tsay, D., and Siegelbaum, S.A. (2007). A role for synaptic inputs at distal dendrites: instructive signals for hippocampal long-term plasticity. Neuron *56*, 866-879.

Empson, R.M., and Heinemann, U. (1995b). The perforant path projection to hippocampal area CA1 in the rat hippocampal-entorhinal cortex combined slice. J Physiol *484 (Pt 3)*, 707-720.

Ferrante, M., Migliore, M., and Ascoli, G.A. (2009). Feed-forward inhibition as a buffer of the neuronal input-output relation. Proc Natl Acad Sci U S A *106*, 18004-18009.

Fitzjohn, S.M., Palmer, M.J., May, J.E., Neeson, A., Morris, S.A., and Collingridge, G.L. (2001). A characterisation of long-term depression induced by metabotropic glutamate receptor activation in the rat hippocampus in vitro. J Physiol *537*, 421-430.

Gabernet, L., Jadhav, S.P., Feldman, D.E., Carandini, M., and Scanziani, M. (2005). Somatosensory integration controlled by dynamic thalamocortical feed-forward inhibition. Neuron *48*, 315-327.

Gantois, I., Vandesompele, J., Speleman, F., Reyniers, E., D'Hooge, R., Severijnen, L.A., Willemsen, R., Tassone, F., and Kooy, R.F. (2006). Expression profiling suggests underexpression of the GABA(A) receptor subunit delta in the fragile X knockout mouse model. Neurobiol Dis *21*, 346-357.

Gibson, J.R., Bartley, A.F., Hays, S.A., and Huber, K.M. (2008). Imbalance of neocortical excitation and inhibition and altered UP states reflect network hyperexcitability in the mouse model of fragile X syndrome. J Neurophysiol *100*, 2615-2626.

Goncalves, J.T., Anstey, J.E., Golshani, P., and Portera-Cailliau, C. (2013). Circuit level defects in the developing neocortex of Fragile X mice. Nat Neurosci *16*, 903-909.

Guetg, N., Seddik, R., Vigot, R., Turecek, R., Gassmann, M., Vogt, K.E., Brauner-Osborne, H., Shigemoto, R., Kretz, O., Frotscher, M.*, et al.* (2009). The GABAB1a isoform mediates heterosynaptic depression at hippocampal mossy fiber synapses. J Neurosci *29*, 1414-1423.

Han, E.B., and Heinemann, S.F. (2013). Distal dendritic inputs control neuronal activity by heterosynaptic potentiation of proximal inputs. J Neurosci *33*, 1314-1325.

Henderson, C., Wijetunge, L., Kinoshita, M.N., Shumway, M., Hammond, R.S., Postma, F.R., Brynczka, C., Rush, R., Thomas, A., Paylor, R.*, et al.* (2012). Reversal of disease-related pathologies in the fragile X mouse model by selective activation of GABAB receptors with arbaclofen. Sci Transl Med *4*, 152ra128.

Izumi, Y., and Zorumski, C.F. (2008). Direct cortical inputs erase long-term potentiation at Schaffer collateral synapses. J Neurosci *28*, 9557-9563.

Klyachko, V.A., and Stevens, C.F. (2006). Excitatory and feed-forward inhibitory hippocampal synapses work synergistically as an adaptive filter of natural spike trains. PLoS Biol *4*, e207.

Kullmann, D.M. (1994). Amplitude fluctuations of dual-component EPSCs in hippocampal pyramidal cells: implications for long-term potentiation. Neuron *12*, 1111-1120.

Laviv, T., Riven, I., Dolev, I., Vertkin, I., Balana, B., Slesinger, P.A., and Slutsky, I. (2010). Basal GABA regulates GABA(B)R conformation and release probability at single hippocampal synapses. Neuron *67*, 253-267.

Lovett-Barron, M., and Losonczy, A. (2014). Behavioral consequences of GABAergic neuronal diversity. Curr Opin Neurobiol *26*, 27-33.

Martin BS, Corbin JG & Huntsman MM. (2014). Deficient tonic GABAergic conductance and synaptic balance in the fragile X syndrome amygdala. J Neurophysiol **112,** 890-902.

Myrick, L.K., Deng, P., Hashimoto, H., Oh, Y.M., Cho, Y., Poidevin, M.J., Suhl, J.A., Visootsak, J., Cavalli, V., Jin, P.*, et al.* (2015). Independent role for presynaptic FMRP revealed by an FMR1 missense mutation associated with intellectual disability and seizures. Proc Natl Acad Sci U S A. *112*:949-56.

Olmos-Serrano, J.L., Paluszkiewicz, S.M., Martin, B.S., Kaufmann, W.E., Corbin, J.G., and Huntsman, M.M. (2010). Defective GABAergic neurotransmission and pharmacological rescue of neuronal hyperexcitability in the amygdala in a mouse model of fragile X syndrome. J Neurosci: *30*, 9929-9938.

Pacey, L.K., Tharmalingam, S., and Hampson, D.R. (2011). Subchronic administration and combination metabotropic glutamate and GABAB receptor drug therapy in fragile X syndrome. J Pharmacol Exp Ther *338*, 897-905.

Paluszkiewicz, S.M., Martin, B.S., and Huntsman, M.M. (2011). Fragile X syndrome: the GABAergic system and circuit dysfunction. Dev Neurosci *33*, 349-364.

Patel, A.B., Hays, S.A., Bureau, I., Huber, K.M., and Gibson, J.R. (2013). A target cell-specific role for presynaptic Fmr1 in regulating glutamate release onto neocortical fast-spiking inhibitory neurons. J Neurosci *33*, 2593-2604.

Patel, A.B., Loerwald, K.W., Huber, K.M., and Gibson, J.R. (2014) Postsynaptic FMRP promotes the pruning of cell-to-cell connections among pyramidal neurons in the L5A neocortical network. J Neurosci *34*, 3413-3418.

Perez-Garci, E., Gassmann, M., Bettler, B., and Larkum, M.E. (2006). The GABAB1b isoform mediates long-lasting inhibition of dendritic Ca2+ spikes in layer 5 somatosensory pyramidal neurons. Neuron *50*, 603-616.

Pouille, F., and Scanziani, M. (2001). Enforcement of temporal fidelity in pyramidal cells by somatic feed-forward inhibition. Science *293*, 1159-1163.

Price, C.J., Scott, R., Rusakov, D.A., and Capogna, M. (2008). GABA(B) receptor modulation of feedforward inhibition through hippocampal neurogliaform cells. J Neurosci *28*, 6974-6982.

Remondes, M., and Schuman, E.M. (2002). Direct cortical input modulates plasticity and spiking in CA1 pyramidal neurons. Nature *416*, 736-740.

Remondes, M., and Schuman, E.M. (2004). Role for a cortical input to hippocampal area CA1 in the consolidation of a long-term memory. Nature *431*, 699-703.

Rotman, Z., Deng, P.Y., and Klyachko, V.A. (2011). Short-term plasticity optimizes synaptic information transmission. J. Neurosci 31(41):14800-9.

Wang, G.X., Smith, S.J., and Mourrain, P. (2014a). Fmr1 KO and Fenobam Treatment Differentially Impact Distinct Synapse Populations of Mouse Neocortex. Neuron *84*, 1273-1286.

Wang, X.S., Peng, C.Z., Cai, W.J., Xia, J., Jin, D., Dai, Y., Luo, X.G., Klyachko, V.A., and Deng, P.Y. (2014b). Activity-dependent regulation of release probability at excitatory hippocampal synapses: a crucial role of fragile X mental retardation protein in neurotransmission. Eur J Neurosci *39*, 1602-1612.

Chapter 3: Dynamic Balance of Excitation and Inhibition Allows for Rapid Modulation of Spiking Probability and Precision

This chapter was co-written by Sarah Wahlstrom Helgren and Vitaly Klyachko in preparation of submission to a peer-review journal.

Neuronal feed-forward inhibitory (FFI) circuits are important for many information-processing functions including filtering and coincidence detection. The specifics of how these circuits operate depends on the balance and timing between the excitatory and inhibitory currents. Because of dynamic changes in both circuit components due to short-term plasticity, this balance changes based on the temporal structure of the incoming spike train. Here, we examined the role of short-term plasticity in the function of FFI circuits in the mouse hippocampus. Understanding of the role of short-term plasticity in this FFI circuit is essential for understanding neuronal encoding. Electrophysiological recordings from the pyramidal layer in the CA1 region of the hippocampus were performed to measure the width and magnitude of the post-synaptic current througout a burst. Additionally, a simulation of the current input during a burst was constructed, with the excitatory component based on our previously published model (Kandaswamy, Deng, Stevens, & Klyachko, 2010). The balance and timing between exciation and inhibition was chosen based on recordings of intact FFI circuit currents in the CA1 pyramidal neurons. The simulation was then used to predict the role of the STP in the FFI circuit functions. To study

spiking behavior, further recordings were performed in a cell-attached mode. Two stimulus electrodes were placed on the Schaffer Collateral (SC) pathway and a coincidence detection protocol was used as described (Pouille & Scanziani, 2001). The probability of spiking and spike jitter were measured for a single stimuli and for the last stimuli in a burst. The probability of observing a spike in response to FFI circuit activation was found to be significantly larger at the end of the high-frequency burst than in response to a single spike. Additionally, an increase in the amount of jitter at the end of the burst was observed. Blocking inhibitory synaptic transmission did not alleviate the increase in spiking probability at the end of the burst, but the increase in the jitter was diminished. Further, combining whole-cell recordings and the simulation model indicated that the dynamic changes in inhibitory component of the FFI circuit during the burst influence the modulation of spiking precision.

3.1 Introduction

Feed-forward inhibitory (FFI) circuits are a canonical unitary circuit found throughout the brain and essential for many fundamental computations (Ang, Carlson, & Coulter, 2005; Chittajallu, Pelkey, & McBain, 2013; Ferrante, Migliore, & Ascoli, 2009; Gabernet et al., 2005; Goudar & Buonomano, 2015; Izumi & Zorumski, 2008; Klyachko & Stevens, 2006; F Pouille & Scanziani, 2001; Remondes & Schuman, 2002; Tsay, Dudman, & Siegelbaum, 2007). It is widely believed that FFI circuits function depends on the fine-tuned balance of excitatory and inhibitory (E/I) circuit components that are tightly time-locked with each other. Yet, how E/I balance modulates FFI circuits function remains poorly understood.

The E/I balance within the FFI circuits is not constant but is rapidly and dynamically modulated by the ongoing activity due to the short-term plasticity (STP) of both excitatory and

inhibitory components. A critical role for STP has been suggested in optimizing information transmission at individual excitatory and inhibitory synapses (Rotman, Deng, & Klyachko, 2011) and in a wide range of information processing operations in a variety of sensory systems (Klug et al., 2012). While the dynamic changes in individual circuit components during spike trains has been extensively studied, how resulting dynamic changes in E/I balance during spike bursts modulate FFI functions remains poorly understood. The only study that previously examined the effects of STP on FFI circuit operations using a simplified case of paired-pulse stimulation concluded that STP not only increases spiking probability but also increases spike precision (evident as reduction in spike jitter) during paired-pulse stimulation (Bartley & Dobrunz, 2015). This reduction in spike jitter, but not increase in spiking probability, were inhibition-dependent, and was attributed to facilitation of disynaptic inhibition. This study, performed at room temperature, is difficult to reconcile with the observations that FFI does not facilitate under physiological conditions (Klyachko & Stevens, 2006). Moreover, an opposite conclusion was reached by another study demonstrating that blocking inhibition in the hippocampal FFI circuits dramatically widened the integration window and decreased spike precision (increase jitter) during coincidence detection (Pouille & Scanziani, 2001). Furthermore, paired-pulse stimulation evokes only the simplest forms of STP, while STP is a complex phenomenon comprising several interdependent forms of dynamic modulation that regulate synaptic function during spike trains, but not apparent during a pair of spikes. The role of STP in regulating the dynamic E/I balance in the FFI circuits therefore remains unclear.

E/I circuit imbalance has been implicated in many neurodevelopmental disorders associated with intellectual disability, including autism, Down, Rett, and Fragile X syndromes (FXS) (Brager & Johnston, 2014; Contractor et al., 2015; Garner & Wetmore, 2012; LeBlanc et

al., 2015; Rubenstein & Merzenich, 2003). Specifically, in FXS, network-level defects in circuit imbalance has been described (Gibson et al., 2008; Gonçalves et al., 2013). We recently uncovered an abnormal STP and excessive excitatory synaptic transmission during spike bursts in hippocampal and cortical neurons of Fmr1 KO mice (Deng, Sojka, & Klyachko, 2011; Deng et al., 2013), a mouse model of FXS, and an E/I imbalance in hippocampal FFI circuits (Deng & Klyachko, 2015; Wahlstrom-Helgren & Klyachko, 2015). How this imbalance affects fundamental circuit operations, spiking probability and precision remains largely unexplored.

Here, we combined experimental measurements and data-driven simulations to study the role of synaptic dynamics in FFI circuit processing, with the focus on integration and spike precision during spike trains. We found that the width of the EPSC dramatically increases during a burst due to the decay of inhibition. We were then able to model the feed-forward circuit and examine the specific roles of excitatory and inhibitory dynamics in both single responses and during a burst of stimuli. In this case, the inhibitory dynamics dominate the width of post-synaptic response. Further, we were able to examine the role of the dynamic changes during a burst on spiking behavior. We found that spiking probability increases at the end of the burst both in the presence and the absence of inhibition, however, the precision of the spiking (measured as jitter) was modulated by the presence of inhibition.

3.2 Methods

Animals and Slice Preparations. Transverse hippocampal slices, 350μm thick, were prepared from mice 18- to 25-days-old using a microtome (Lecia, Germany). Mice were obtained from The Jackson Laboratory (Bar Harbor, ME, USA). Slicing was performed in an ice-cold bath solution of artificial cerebral spinal fluid: 125mM NaCl, 25mM $NaHCO_3$, 2.5mM KCl, 1.25mM

NaH_2PO_4, 10mM glucose, 0.5mM CaCl2, 4.0mM $MgCl_2$. Slices recovered in a heated chamber (33°C) for ~1hr, and then were kept at room temperature until use (~23°C).

Electrophysiology. Data collection was performed using an Axopatch 200B amplifier (Molecular Devices, Sunnyvale, CA, USA) and custom software written in LabView (National Instruments Corp., Austin, TX, USA) in conjunction with a National Instruments A/D board to filter (at 2kHz) and digitize the signal. A Nikon E600N microscope with mounted differential interference contrast optics was used to visually identify CA1 pyramidal cells. All recordings were performed under profusion of a bath solution: 125 mM NaCl, 25mM $NaHCO_3$, 2.50mM KCl, 1.25mM NaH_2PO_4, 10mM glucose, 2.0mM $CaCl_2$, 1.0mM $MgCl_2$, 50μM AP-5. During spiking experiments, 2 μM of CGP55845 was also added to the bath to block $GABA_B$ receptors. The temperature of the bath solution was maintained between 33-34°C throughout the duration of all recordings. All stimuli are evoked using extracellular monopolar electrodes.

Whole-cell recordings were performed using a pipette solutions consisting of (in mM): 140 K-gluconate, 0.5 EGTA, 2 $MgCl_2$, 4 NaCl, 3 MgATP, 0.3 LiGTP, 15 HEPES, and 1 QX314 (pH 7.3). Cells were held at a reversal potential of -55mV during these recordings. Cell attached recordings were performed using a pipette solution identical to that of the bath solution.

Spiking Experiments. Each pathway was stimulated 15-25 times to establish the probability of evoking a post-synaptic spike. The pathways were either activated simultaneously with a single "paired" stimulus each, or were applied to one electrode and a single stimulus was delivered to the other; the single/burst stimuli were alternated between the two electrodes throughout the experiment.

Data Analysis. Spiking probability following a burst was normalized to the probability of spiking following a single stimuli for the corresponding time delay. This approach was employed to avoid any artifacts that may arise from a shift in the baseline spiking probability due to long-term plasticity or intrinsic cellular changes. Jitter was analyzed on a cell by cell bases and then weighted as an average into the group based on the square of the number of spikes observed in the cells over the square of the total number of spikes observed.

Modeling of Traces. Recordings of responses to the feed-forward stimulus and the excitatory only stimulus were used to create the model traces. For each cell the excitatory trace was subtracted from the feed-forward inhibitory response to generate the inhibitory trace. Trace shapes were created by averaging responses across all cells. Using the excitatory and inhibitory traces independently, combinations of different ratios could be explored. The delay between the excitatory and inhibitory traces was chosen based on the average delay between excitation and inhibition in the recorded data.

Modeling of Short-term Plasticity. The model used for the short-term plasticity of the excitatory synapse was previously developed by the lab (Kandaswamy et al., 2010). The model of inhibitory short-term plasticity is made up of two depressive components and one recovery component, τ. The first depression term, d_1, is based on the paired-pulse depression data. The second depression term, d_2, is a constant.

$$A(t+1) = d_1 d_2 \left\{ A(t) + \frac{(1 - A(t) d_1)}{\tau} \right\} \quad \textit{Eq. 3.1}$$

Where dt is the time between the stimuli, and A(t) is the value of the synaptic strength and is limited to values between 0 and 1. The values of τ and d_2 were chosen to best fit the constant frequency and natural spike train IPSP data (Fig. 3.3).

Modeling of Feed-Forward Inhibition. Combining the traces and plasticity measurements a model of a feed-forward circuit to a continuous train of stimuli was implemented. To do this, a waveform that was 100ms long was created for each specific stimuli and then added to the total trace. This addition is to account for the post-synaptic temporal integration that occurs.

3.3 Results

3.3.1 Short-term depression of disynaptic inhibition causes EPSC broadening during bursts in hippocampal feed-forward circuits

Previous studies performed at room temperature (Bartley & Dobrunz, 2015), attributed the increase in spike probability observed with a paired-pulse stimulation to the facilitation of the disynaptic inhibition at short ISIs (<200ms). We found here that both the direct inhibition and the disynaptic inhibition of the hippocampal FFI circuit do not facilitate under physiological conditions (Fig. 3.6), but rather exhibit short-term depression in agreement with earlier studies (Klyachko & Stevens, 2006). To further investigate dynamic changes in the FFI circuit during bursts, we performed whole-cell recordings of synaptic dynamics evoked by activation of the FFI circuit in the voltage-clamped CA1 neurons. Responses consisted of a canonical EPSC/IPSC pair typical of FFI circuit activation and was recorded for single paired-stimulus and a paired stimulus at the end of 18 stimuli natural burst train (Fig. 3.1A) in the absence (5μM Gabazine) and presence of inhibition. Comparison of the single-stimulus responses and responses during the burst revealed decay of di-synaptic IPSC and increase in EPSC amplitudes (Fig. 3.1B,C) and a concomitant broadening of EPSP (Fig. 3.1B,D). The increase in EPSC amplitude was

observed whether inhibition was present or not, and was in fact larger in the presence of inhibition (Fig. 3.1C). We found previously that this effect is caused by a combination of short-term enhancement of excitation and concomitant depression of inhibition (Klyachko & Stevens, 2006). Importantly, here we found that EPSP broadening was no longer evident when inhibition was blocked (Fig. 3.2D, Exc + Inh: 2.8 ± 0.5, Exc Only: 1.0 ± 0.03, n = 9; p = 0.006; Mann-Whitney U test, here and throughout), suggesting that dynamics of inhibition also controls EPSC width during trains.

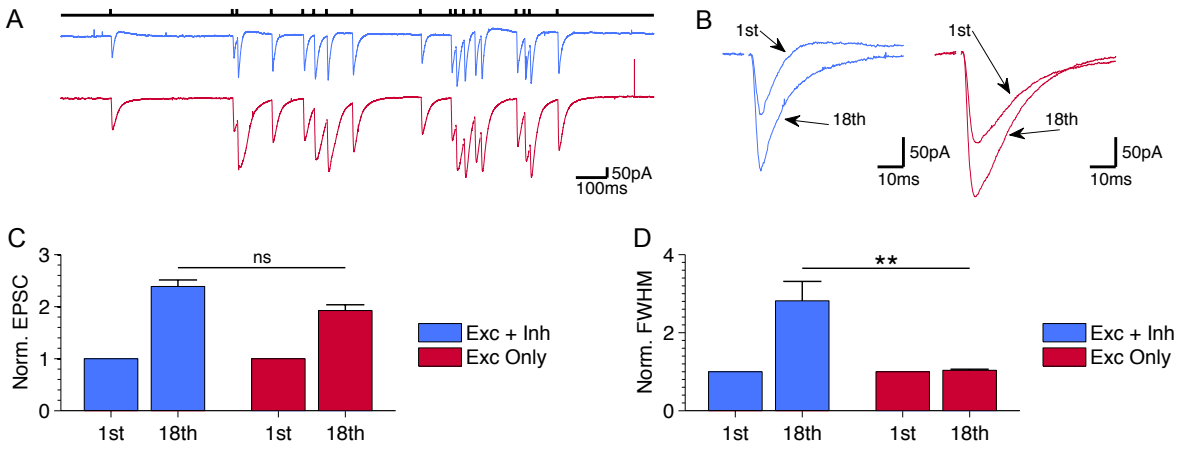

Figure 3.1. Inhibition decay is responsible for width change of the EPSC

A. Example of trace of a natural burst with (blue) and without (red) inhibition. Stimulus artifacts have been removed (here and throughout) for clarity.

B. Zoom and overlay of first and last pulse of the burst with (blue) and without (red) inhibition. Stimulus artifacts have been removed (here and throughout) for clarity.

C. Normalized EPSC of the first and last pulse of the burst with and without inhibition.

D. Normalized full-width, half-maximum (FWHM) for the first and last pulse of the burst with and without inhibition.

**p<0.01, *p<0.05, ns – not significant.

3.3.2 Simulations of the feed-forward circuit responses support the critical role of inhibition in regulating EPSC width

To examine quantitatively how STP of individual circuit components regulate dynamic E/I balance and contribute to FFI circuit responses during bursts, we employed a simple computational approach to reconstruct FFI circuit responses and to simulate its dynamics based on experimental recordings of individual components alone and the timing between the components. We then used this approach to predict how dynamic changes in E/I balance during bursts alter FFI circuit responses and verified these predictions experimentally.

First, we determined baseline responses of each FFI circuit component to a single stimulus using whole-cell recordings in CA1 pyramidal cells (Fig. 3.2B). The EPSC/IPSC sequences were evoked by single SC stimulation and recorded first at -55mV, a potential at which both FFI circuit components are evident, and then at -80mV, near Cl^- reversal potential, when only EPSC is evident Fig. 3.2B). The di-synaptic IPSC was then extracted from these traces by subtracting the -80mV trace from the -55mV trace (Pouille & Scanziani, 2001). EPSC/IPSC peak ratio, the time to peak of EPSC and IPSC and E-I peak delay was determined for each cell (Fig. 3.2C, D). The EPSC and IPSC traces were averaged across all cells (Fig. 3.2E) and combined to construct the average FFI circuit response to a single stimulus based on average E/I ratio and E-I delay (Fig. 3.2F).

We then used these simulated traces to examine how the E/I balance in the FFI circuit influences the width of the EPSC, by systematically varying the E/I ratio. First, varying relative amount of inhibition while holding excitation constant (Fig. 3.2G, I) strongly affected the width of the EPSC, while causing little change in EPSC magnitude. In contrast, varying the amount of

excitation while holding inhibition constant caused marked changes in magnitude of EPSC and small changes in EPSC width (Fig. 3.2H, J). This result supports the above findings of the differential roles of excitation and inhibition in altering EPSC properties in the FFI circuit response and further supports the predominate role of inhibition in altering EPSC width.

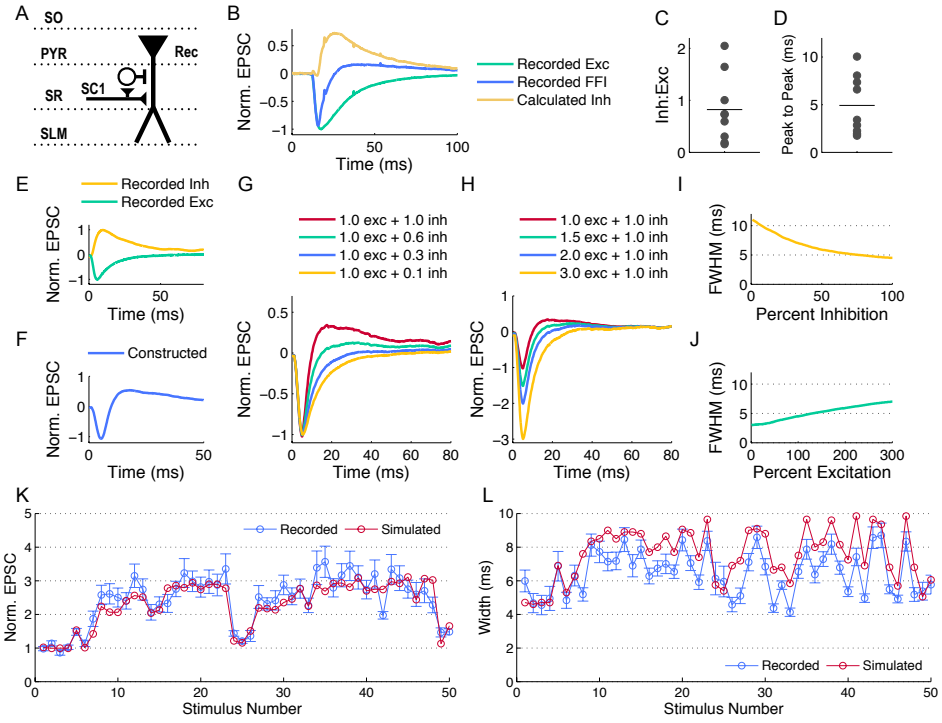

Figure 3.2. The role of excitation/inhibition balance in determining the width of the EPSC

A. Schematic of stimulation protocol. Abbreviations denote hippocampal layers.

B. Example trace showing how excitation is subtracted from the FFI trace to extract the inhibitory component. Stimulus artifacts have been removed (here and throughout) for clarity.

C. Inhibition to excitation ratio as measured in 7 cells, line represents the average.

D. Time between excitatory and inhibitory peaks as measured in 7 cells, line represents the average.

E. Example traces of recorded excitation and recorded inhibition that are used to construct the feed-forward inhibitory trace.

F. Constructed feed-forward inhibitory trace.

G. Examples of constructed traces when the amount of inhibition is varied.

H. Examples of constructed traces when the amount of excitation is varied.

I. Influence of the inhibition on the width of the EPSC, measured as full-width at half-maximum (FWHM).

J. Influence of excitation magnitude on the width of the EPSC

K. Measurement of normalized peak EPSC from recorded and simulated natural spike train.

L. Measurement of width from recorded and simulated natural spike train.

3.3.3 The role of STP in modulating E/I balance during bursts in a feed-forward circuit

To extend these simulations to a case of a burst, we incorporated the dynamic changes of the individual circuit components, again based on experimental recordings of synaptic dynamics in this circuit. To establish inhibitory synapse dynamics, IPSCs were recorded from CA1 pyramidal cells in response to SC pathway stimulation with a set of constant frequency trains from 2Hz to 80Hz in the absence of excitation (APV (50μM) and DNQX (10μM)) (Fig. 3.3A). A three-parameter model incorporating fast depression, slow depression, and a recovery processes was then fit to the average IPSC values determined from these recordings. Model performance was evaluated by predicting a response to a random spike train (Fig. 3.3B).

Previous findings indicated that excitatory synapses from CA3 PCs onto CA1 inhibitory hippocampal interneurons are highly reliable and therefore are expected to exhibit a certain degree of short-term depression during trains that would combine with the depression of their inhibitory synapses to result in overall short-term depression of di-synaptic inhibition. This notion however, has been challenged recently by a recent study suggesting that instead that di-synaptic inhibition exhibits strong paired-pulse facilitation that plays a major role in FFI circuit properties (Bartley & Dobrunz, 2015). Therefore care was taken to specifically examine dynamics of both direct mono-synaptic inhibition and disynaptic inhibition in the intact FFI circuit. In all cases, paired-pulse stimulation led to paired-pulse depression at various ISIs under physiological conditions (Fig. 3.6). Further, comparison of dynamic changes in mono- and di-synaptic inhibition indicated that the inhibitory dynamics in the FFI circuit is dominated by the short-term depression of mono-synaptic inhibition with small additional contribution from depression of excitatory input onto interneurons.

Finally we combined the above model of inhibitory plasticity, with the existing model of an excitatory SC synapse STP we developed previously (Kandaswamy et al., 2010), to construct averaged simulated EPSCs during a train. Inputs were assumed to temporally sum in the post-synaptic cell. The performance of the model was evaluated by comparison with our recordings of synaptic currents from the intact FFI circuit. The simulation was able to capture the dynamic changes that occur in both magnitude and width of EPSC with the close agreement with the experimental recordings (Fig. 3.2K, L). Because the simulations were created in assumption that the excitatory inputs to the FFI interneurons are reliable, the close agreement between simulated and experimentally observed dynamics provide further support for the notion that the excitatory inputs to the FFI interneurons do not strongly contribute to dynamic changes in the FFI circuit during bursts in contrast to the previous study (Bartley & Dobrunz, 2015).

This simulation is advantageous because it allows for the testing of the role STP of each excitation and inhibition independently in a way that could not be achieved experimentally. A burst of 40 stimuli at 40Hz was chosen to examine the simulated circuit behavior. First, all STP was removed from the model and changes simply due to post-synaptic integration were explored (Fig. 3.4Ai-Aiii). In the absence of any synaptic dynamics we observed a slight increase in the width of each EPSC throughout the train (Fig. 3.4Aiii). Next, the excitatory synapse STP was implemented, but the inhibitory synaptic strength remained constant. In this case, a step-wise increase in EPSC width is evident that slowly recovered following the train with the same time course as augmentation decay (Fig. 3.4Biii). Then, in a similar way, the excitation was held constant and the inhibitory plasticity was implemented (Fig. 3.4Ci-Ciii), larger changes in the EPSC width were observed with the extent of the changes dependent on the length of the stimulus train. Finally, the model was tested with STP at both excitatory and inhibitory synapses

present (Fig. 3.4Di-Diii) demonstrating an increase in the width throughout the train. We note however, that the observed changes in width are not a linear summation of the changes in width seen for each type of synapse independently.

Together these simple simulations indicate that EPSC width is dynamically modulated during trains predominately due to STP (depression) of inhibition with the smaller contribution from enhancement of excitation.

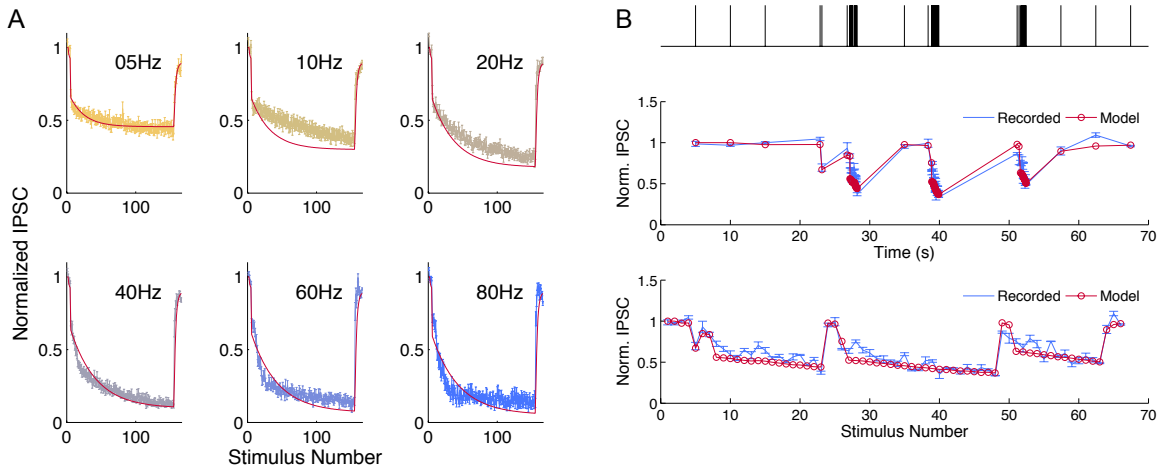

Figure 3.3. Model of synaptic depression in an inhibitory synapse

A. Normalized peak IPSCs of the model (red) and from recorded neurons at various frequencies.

B. Model response (red) compared to recorded response (blue) during a natural spike train. Top scheme shows the natural burst sequence.

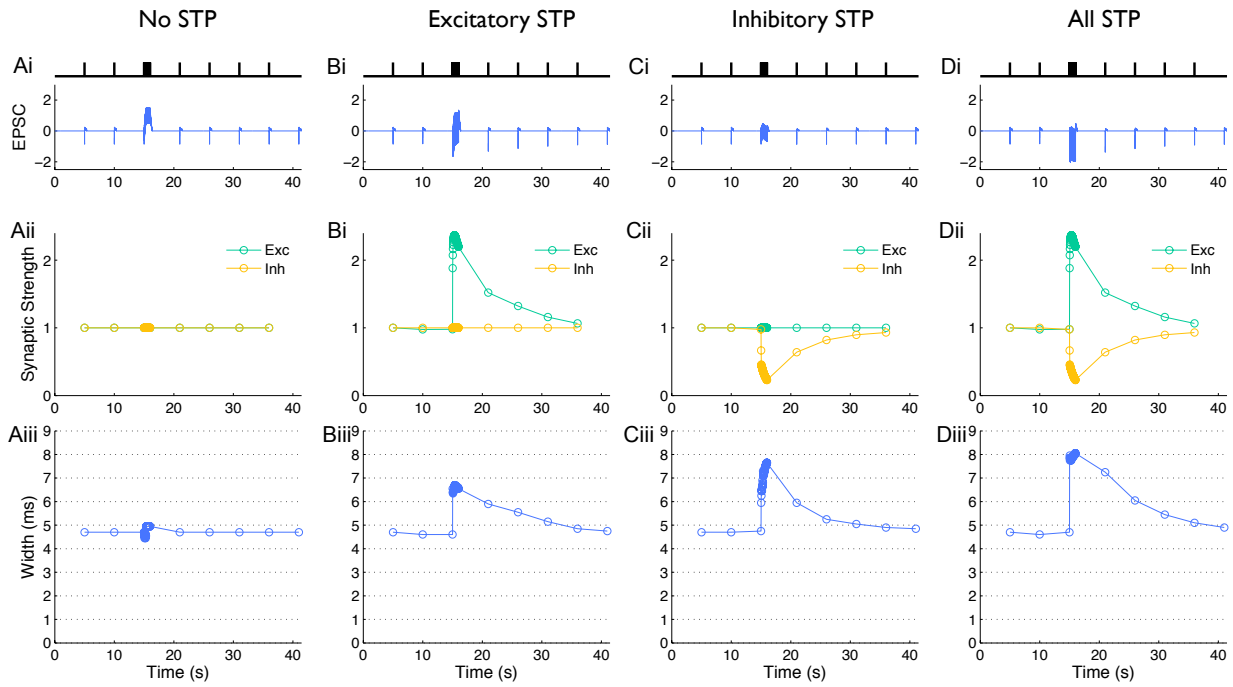

Figure 3.4. The role of short-term plasticity in determining the width of the EPSC during a burst

Ai. Trace of stimulated response when no short-term plasticity (STP) is present.

Aii. Synaptic strength used in simulation when no STP is present.

Aiii. Width of each pulse in the train as measured during simulation when no STP is present.

Bi, Bii, Biii. Same as A, B, C, when only excitatory STP is present.

Ci, Cii, Ciii. Same as A, B, C, when only inhibitory STP is present.

Di, Dii, Diii. Same as A, B, C, when both excitatory and inhibitory STP are present.

3.3.4 Distinct roles of excitatory and inhibitory dynamics in modulating spiking probability and precision during bursts in feed-forward hippocampal circuits

While the role of E/I balance in basic FFI circuit operations is well established, how rapid dynamic changes caused by STP during spike bursts affects fundamental circuit operations remains poorly understood. To approach this question, we used a basic coincidence detection paradigm (Pouille & Scanziani, 2001) and compared coincidence detection features of the hippocampal FFI circuit for single spikes and during bursts. Two stimulus electrodes were placed in the SR on either side from the CA1 pyramidal cell being recorded from (Fig 3.5A, B) and the stimulus intensities were set to be below the threshold for evoking a spike in the post-synaptic cell when either pathway was activated alone. We then compared the probability of evoking a spike in response to single paired stimuli in the two pathways with the same paired stimuli applied at the end of a 15-stimulus burst at 20 Hz. In addition, the timing between the paired stimuli (ΔT) was measured at 0ms and 10ms. Spiking probability for a burst was normalized to the probability measured for the single paired-stimuli at the same ΔT. This analysis revealed that spiking probability was significantly increased (~2 times) at the end of the burst compared to single spikes at $\Delta T = 0$ (Fig 3.5C). The effect of the burst on spiking probability decayed rapidly with increase in ΔT (Fig. 3.5C). This result suggests that dynamic synaptic changes during burst have a major influence on the spiking probability during coincidence detection task.

The inhibitory component of the FFI circuit has been implicated in controlling temporal fidelity of the target cell spiking (Pouille & Scanziani, 2001). We therefore examined the role of inhibition in setting the strength of coincidence detection during bursts, using the same paradigm

as above in the presence of Gabazine (5μM) (Fig. 3.5C). Surprisingly, we found that blocking inhibition had no influence on the dynamic change in spiking probability at the end of the bursts (Fig. 3.5C).

We next examined how bursts affect the spike precision, by analyzing the jitter of individual spikes relative to the average spike time for each cell, for single paired-stimuli and for the same paired stimuli at the end of the 15-stimulus burst at 20 Hz. Jitter increased 2-fold at the end of the bursts compared to single paired stimuli (Fig. 3.5D, E), indicating a reduction in spike precision. Importantly, this increase in spike jitter during bursts was strongly, but not completely, reduced by block of inhibition (Fig. 3.5G, H).

Together these results suggest that inhibitory component modulates the spike precision, while excitatory component predominately modulates spike probability in the hippocampal FFI circuits during the trains with smaller additional influence on spike precision.

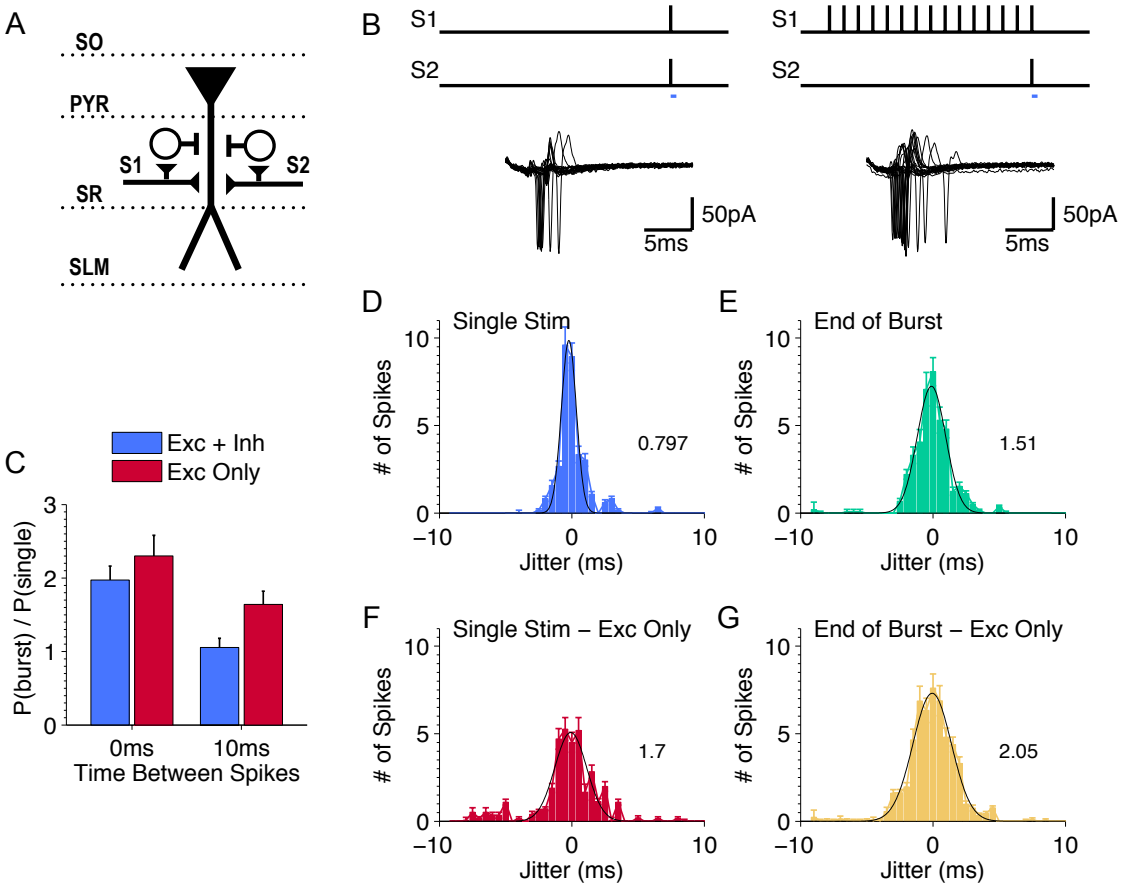

Figure 3.5. Jitter is modulated by the decay of inhibition during the burst

A. Schematic of stimulation protocol. Abbreviations denote hippocampal layers.

B. Stimulus delivery scheme and example of resulting cell response.

C. Normalized probability of observing a spike at the end of the burst. Time between spikes refers the time between last input of S1 and input of S2.

D. Jitter that occurs when a single stimulus is delivered to S1.

E. Jitter that occurs when a burst of stimuli are delivered to S1.

F. Same as C, with both $GABA_A$ and $GABA_B$ receptors blocked by Gabazine and CGP55845, respectively.

G. Same as D, with inhibition blocked.

H. Same as E, with inhibition blocked.

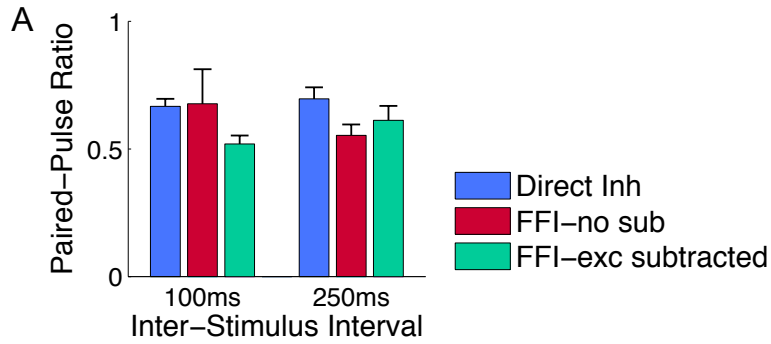

Figure 3.6. Paired-pulse depression in inhibitory synapses

A. Paired-pulse results for different inhibitory set-ups.

3.4 Discussion

In this study, we sought to examine the role of STP in the dynamical behavior of feed-forward circuits and to further probe the implications it has for circuit output during bursts. Our experimental measurements and simulations suggest that the short-term depression of feed-forward inhibition is responsible for changes in width of EPSC seen during a burst, while dynamics of excitation is predominately responsible for changes in amplitude of the EPSC. Moreover, dynamics of inhibition modulated the spike precision during burst but not the changes in spiking probability, which is attributed to the dynamics of the excitation.

Coincidence detection cell-attached experiments revealed that the dynamics of feed-forward inhibition play a critical role in the modulation of spiking precision. The changes in jitter seen between a single stimulus and a burst of stimuli further support the ideas previously presented (Pouille & Scanziani, 2001), showing that a decrease in spiking precision is associated with the decrease in inhibition. This relationship is attributed to the increase in rise time of the excitatory response that occurs as a result of blocking of inhibition. Further, others using different approaches showed that increases in tonic GABA decrease the membrane time constant and improve spike precision (Wlodarczyk et al., 2013). Overall, our results provide further evidence of this relationship. The novel and unexpected finding of our study is that blocking inhibition strongly reduces changes in spike jitter during bursts.

It is worth noting we did not observe an increase in the width of the coincidence detection window with the decay of inhibition, as may have been expected given previous work (Pouille & Scanziani, 2001). However, because only one of the stimulated pathways receives the burst stimulus it is plausible that there is some amount of inhibition activated by the second pathway.

This may be responsible for maintaining the narrow coincidence detection window while unable to fully maintain the spiking precision.

It was recently implied that there is short-term facilitation that happens in inhibitory synapses contributing to the role of short-term plasticity in coincidence detection during paired-pulse stimuli (Bartley & Dobrunz, 2015). However, it should be noted that these experiments were performed at room temperature, and specifically in the case of a coincidence detection protocol, correct physiological temperature is critical. Because temperature can influence the speed of propagation of neural signals (König, Engel, Roelfsema, & Singer, 1996), it is also critical to short-term plasticity dynamics (Klyachko & Stevens, 2006). Additionally, we did not observe paired-pulse facilitation of inhibition in any of our measurements (Fig. 3.6). Finally, our simulation results further support that paired-pulse depression rather than facilitation of inhibition occurs at physiological temperatures. As a result, paired-pulse facilitation of inhibition is unlikely to be a mechanism underlying changes observed here under physiologically relevant conditions.

Our recordings of feed-forward circuit dynamics are corroborated by a computational simulation of the circuit behavior. To our knowledge, this is the first attempt to examine the roles of each type of plasticity within the feed-forward circuit using a model that is built from experimental data. Although there are many other models of short-term plasticity (Hennig, 2013; Kandaswamy et al., 2010) or of feed-forward inhibition (Ferrante et al., 2009; George, Lyons-Warren, Ma, & Carlson, 2011; Jang & Kwag, 2012; Keck, Savin, & Lücke, 2012; Saraga, Balena, Wolansky, Dickson, & Woodin, 2008; Zalay & Bardakjian, 2006; Zhou, Tao, & Zhang, 2012), surprisingly, to our knowledge, no previous studies have focused on the influence of the plasticity on the width of the post-synaptic response and its relationship with the circuit output.

We note, however, that our computational work is limited by the assumption of the relationship between the size and shape of the EPSC and the spiking behavior. There are many contributing factors to the spiking behavior of a neuron—dendritic integration, intrinsic plasticity, neuronal dynamics—that we did not consider. For example, the reversal potential for Cl^- has previously been shown to be essential in regulation of spiking activity (Saraga et al., 2008). Previous work has attributed the rise time of the EPSC/EPSP to be correlated with the increase in jitter by using current-clamp recordings (Pouille & Scanziani, 2001; Wlodarczyk et al., 2013), however, the association between the width of the post-synaptic response and the jitter has not, to our knowledge, been examined experimentally. Future work will be needed to examine this relationship in detail. Another limiting consideration in the simulation work presented here is the absence of a probabilistic synaptic release parameter, which represents the unreliability of the synapse. Unreliability limits the amount of information a neuron can transmit (Schreiber, Fellous, Whitmer, Tiesinga, & Sejnowski, 2003). Because our simulation is of an averaged neuronal response, it does not take unreliability into account and therefore misses this important aspect of the neuronal processing.

The feed-forward inhibitory circuit is a dynamical system, and importantly, because of both short-term plasticity and long-term plasticity it has dynamics that occur on many time scales. This range of time scales implies that there may not be a stable sink point of the system. Spike train input needed to generate the same output changes in time because of this non-stationarity and the plasticity of the intrinsic excitability of the neuron. This implies that in contrast to previous thinking (Rieke, Warland, Steveninck, & Bialek, 1999), the delivery of two identical stimuli may not produce the same spike response. This work aligns with previous findings of the importance of the sequence of inter-spike intervals (Rieke et al., 1999) and extends that

importance beyond a single synapse and to the microcircuit level during a burst. The presence of a burst allows for the temporary manipulation of this balance allowing the circuit to increase its information transfer by increasing the probability that a coincidence will be detected in the post-synaptic cell. However, this increase in information transfer comes at a cost, as the precision of the spike timing is decreased.

Because altered balance of excitation and inhibition and circuit hyperexcitability have been shown to be critical in many disease states, one future direction of this study is to examine the dynamic changes in feed-forward circuit behavior and its influence on spike probability and precision in a disease state. Specifically, in Fragile X Syndrome where hyperexcitability is known, the impact of the hyperexcitability on information processing of the microcircuits has only minimally been explored (Rubenstein & Merzenich, 2003; Wahlstrom-Helgren & Klyachko, 2015).

References

Anderson, P., Morris, R., Amaral, D., Bliss, T., & O'Keefe, J. (2006). *The Hippocampus Book*. Oxford Scholarship Online. Retrieved from http://www.oxfordscholarship.com/view/10.1093/acprof:oso/9780195100273.001.0001/acprof-9780195100273-chapter-3?print

Ang, C. W., Carlson, G. C., & Coulter, D. a. (2005). Hippocampal CA1 circuitry dynamically gates direct cortical inputs preferentially at theta frequencies. *Journal of Neuroscience*, *25*(42), 9567–80. doi:10.1523/JNEUROSCI.2992-05.2005

Bartley, A. F., & Dobrunz, L. E. (2015). Short-term plasticity regulates the excitation / inhibition ratio and the temporal window for spike integration in CA1 pyramidal cells. *European Journal of Neuroscience*, *41*(February), 1402–1415. doi:10.1111/ejn.12898

Bear, M. F., Huber, K. M., & Warren, S. T. (2004). The mGluR theory of fragile X mental retardation. *Trends in Neurosciences*, *27*(7), 370–377. doi:10.1016/j.tins.2004.04.009

Blitz, D. M., & Regehr, W. G. (2005). Timing and specificity of feed-forward inhibition within the LGN. *Neuron*, *45*(6), 917–28. doi:10.1016/j.neuron.2005.01.033

Brager, D. H., & Johnston, D. (2014). Channelopathies and dendritic dysfunction in fragile X syndrome. *Brain Research Bulletin*, *103*, 11–17. doi:10.1016/j.brainresbull.2014.01.002

Buzsáki, G., & Moser, E. I. (2013). Memory, navigation and theta rhythm in the hippocampal-entorhinal system. *Nature Neuroscience*, *16*(2), 130–8. doi:10.1038/nn.3304

Chittajallu, R., Pelkey, K. A., & McBain, C. J. (2013). Neurogliaform cells dynamically regulate somatosensory integration via synapse-specific modulation. *Nature Neuroscience*, *16*(1), 13–15. doi:10.1038/nn.3284

Contractor, A., Klyachko, V. A., & Portera-Cailliau, C. (2015). Altered Neuronal and Circuit Excitability in Fragile X Syndrome. *Neuron*, *87*(4), 699–715. doi:10.1016/j.neuron.2015.06.017

D'Hulst, C., Heulens, I., Van der Aa, N., Goffin, K., Koole, M., Porke, K., … Kooy, R. F. (2015). Positron Emission Tomography (PET) Quantification of GABAA Receptors in the Brain of Fragile X Patients. *Plos One*, *10*(7), e0131486. doi:10.1371/journal.pone.0131486

Deng, P., & Klyachko, V. A. (2015). Genetic Upregulation of BK Channel Activity Normalizes Multiple Synaptic and Circuit Defects in a Mouse Model of Fragile X Syndrome

Departments of Cell Biology and Physiology , Biomedical Engineering , CIMED , Washington University , St . Louis , MO ; *Journal of Physiology*, 0–26. doi:10.1113/JP271031.This

Deng, P., Rotman, Z., Blundon, J. a, Cho, Y., Cui, J., Cavalli, V., … Klyachko, V. a. (2013). FMRP regulates neurotransmitter release and synaptic information transmission by modulating action potential duration via BK channels. *Neuron*, *77*(4), 696–711. doi:10.1016/j.neuron.2012.12.018

Deng, P., Sojka, D., & Klyachko, V. a. (2011). Abnormal Presynaptic Short-Term Plasticity and Information Processing in a Mouse Model of Fragile X Syndrome. *Journal of Neuroscience*, *31*(30), 10971–10982. doi:10.1523/JNEUROSCI.2021-11.2011

Ferrante, M., Migliore, M., & Ascoli, G. a. (2009). Feed-forward inhibition as a buffer of the neuronal input-output relation. *Proceedings of the National Academy of Sciences of the United States of America*, *106*(42), 18004–9. doi:10.1073/pnas.0904784106

Gabernet, L., Jadhav, S. P., Feldman, D. E., Carandini, M., & Scanziani, M. (2005). Somatosensory Integration Controlled by Dynamic Thalamocortical Feed-Forward Inhibition. *Neuron*, *48*(2), 315–327. doi:10.1016/j.neuron.2005.09.022

Garner, C., & Wetmore, D. (2012). Synaptic Plasticity (Vol. 970, pp. 553–572). doi:10.1007/978-3-7091-0932-8

George, A. a, Lyons-Warren, A. M., Ma, X., & Carlson, B. a. (2011). A diversity of synaptic filters are created by temporal summation of excitation and inhibition. *The Journal of Neuroscience : The Official Journal of the Society for Neuroscience*, *31*(41), 14721–34. doi:10.1523/JNEUROSCI.1424-11.2011

Gibson, J. R., Bartley, A. F., Hays, S. a, & Huber, K. M. (2008). Imbalance of neocortical excitation and inhibition and altered UP states reflect network hyperexcitability in the mouse model of fragile X syndrome. *Journal of Neurophysiology*, *100*(5), 2615–26. doi:10.1152/jn.90752.2008

Gonçalves, J. T., Anstey, J. E., Golshani, P., & Portera-Cailliau, C. (2013). Circuit level defects in the developing neocortex of Fragile X mice. *Nature Neuroscience*, *16*(7), 903–909. doi:10.1038/nn.3415

Goudar, V., & Buonomano, D. V. (2015). A model of order-selectivity based on dynamic changes in the balance of excitation and inhibition produced by short-term synaptic plasticity. *Journal of Neurophysiology*, *113*(2), 509–523. doi:10.1152/jn.00568.2014

Hennig, M. H. (2013). Theoretical models of synaptic short term plasticity. *Frontiers in Computational Neuroscience*, *7*(April), 45. doi:10.3389/fncom.2013.00045

Hitti, F. L., & Siegelbaum, S. a. (2014). The hippocampal CA2 region is essential for social memory. *Nature*, *508*(7494), 88–92. doi:10.1038/nature13028

Izhikevich, E. (2010). *Dynamical Systems in Neuroscience*. Cambridge, MA: MIT Press.

Izumi, Y., & Zorumski, C. F. (2008). Direct cortical inputs erase long-term potentiation at Schaffer collateral synapses. *The Journal of Neuroscience : The Official Journal of the Society for Neuroscience*, *28*(38), 9557–63. doi:10.1523/JNEUROSCI.3346-08.2008

Jang, H. J., & Kwag, J. (2012). GABAA receptor-mediated feedforward and feedback inhibition differentially modulate hippocampal spike timing-dependent plasticity. *Biochemical and Biophysical Research Communications*, *427*(3), 466–72. doi:10.1016/j.bbrc.2012.08.081

Kandaswamy, U., Deng, P.-Y., Stevens, C. F., & Klyachko, V. a. (2010). The role of presynaptic dynamics in processing of natural spike trains in hippocampal synapses. *The Journal of Neuroscience : The Official Journal of the Society for Neuroscience*, *30*(47), 15904–14. doi:10.1523/JNEUROSCI.4050-10.2010

Keck, C., Savin, C., & Lücke, J. (2012). Feedforward inhibition and synaptic scaling--two sides of the same coin? *PLoS Computational Biology*, *8*(3), e1002432. doi:10.1371/journal.pcbi.1002432

Kleschevnikov, A. M., Belichenko, P. V, Faizi, M., Jacobs, L. F., Htun, K., Shamloo, M., & Mobley, W. C. (2012). Deficits in Cognition and Synaptic Plasticity in a Mouse Model of Down Syndrome Ameliorated by GABA B Receptor Antagonists, *32*(27), 9217–9227. doi:10.1523/JNEUROSCI.1673-12.2012

Klug, A., Borst, J. G. G., Carlson, B. A., Kopp-Scheinpflug, C., Klyachko, V. A., & Xu-Friedman, M. A. (2012). How Do Short-Term Changes at Synapses Fine-Tune Information Processing? *Journal of Neuroscience*, *32*(41), 14058–14063. doi:10.1523/JNEUROSCI.3348-12.2012

Klyachko, V. a, & Stevens, C. F. (2006). Excitatory and feed-forward inhibitory hippocampal synapses work synergistically as an adaptive filter of natural spike trains. *PLoS Biology*, *4*(7), e207. doi:10.1371/journal.pbio.0040207

König, P., Engel, A. K., Roelfsema, P. R., & Singer, W. (1996). Coincidence detection or temporal integration. The role of the cortical neuron revisited. *Trends Neurosci.*, *19*(4), 130–137.

LeBlanc, J. J., DeGregorio, G., Centofante, E., Vogel-Farley, V. K., Barnes, K., Kaufmann, W. E., … Nelson, C. A. (2015). Visual evoked potentials detect cortical processing deficits in Rett syndrome. *Annals of Neurology*, n/a–n/a. doi:10.1002/ana.24513

Mailick, M. R., Hong, J., Rathouz, P., Baker, M. W., Greenberg, J. S., Smith, L., & Maenner, M.

(2014). Low-normal FMR1 CGG repeat length: phenotypic associations. *Frontiers in Genetics*, *5*(September), 1–8. doi:10.3389/fgene.2014.00309

Martin, B. S., Corbin, J. G., & Huntsman, M. M. (2014). Deficient tonic GABAergic conductance and synaptic balance in the Fragile-X Syndrome Amygdala. *Journal of Neurophysiology*, *3*(303), 890–902. doi:10.1152/jn.00597.2013

Moser, E. I., Kropff, E., & Moser, M.-B. (2008). Place cells, grid cells, and the brain's spatial representation system. *Annual Review of Neuroscience*, *31*, 69–89. doi:10.1146/annurev.neuro.31.061307.090723

Mullard, A. (2015). Fragile X disappointments upset autism ambitions. *Nature Reviews Drug Discovery*, *14*(3), 151–153. doi:10.1038/nrd4555

Neuhofer, D., Henstridge, C. M., Dudok, B., Sepers, M., Lassalle, O., Katona, I., & Manzoni, O. J. (2015). Functional and structural deficits at accumbens synapses in a mouse model of Fragile X. *Frontiers in Cellular Neuroscience*, *9*(March), 1–15. doi:10.3389/fncel.2015.00100

Pollard, M., Varin, C., Hrupka, B., Pemberton, D. J., Steckler, T., & Shaban, H. (2012). Synaptic transmission changes in fear memory circuits underlie key features of an animal model of schizophrenia. *Behavioural Brain Research*, *227*(1), 184–93. doi:10.1016/j.bbr.2011.10.050

Pouille, F., Marin-Burgin, A., Adesnik, H., Atallah, B. V, & Scanziani, M. (2009). Input normalization by global feedforward inhibition expands cortical dynamic range. *Nature Neuroscience*, *12*(12), 1577–85. doi:10.1038/nn.2441

Pouille, F., & Scanziani, M. (2001). Enforcement of temporal fidelity in pyramidal cells by somatic feed-forward inhibition. *Science (New York, N.Y.)*, *293*(5532), 1159–63. doi:10.1126/science.1060342

Remondes, M., & Schuman, E. M. (2002). Direct cortical input modulates plasticity and spiking in CA1 pyramidal neurons. *Nature*, *416*(6882), 736–40. doi:10.1038/416736a

Rieke, F., Warland, D., Steveninck, R., & Bialek, W. (1999). *Spikes*. Cambridge, MA: MIT Press.

Rotman, Z., Deng, P.-Y., & Klyachko, V. a. (2011). Short-Term Plasticity Optimizes Synaptic Information Transmission. *Journal of Neuroscience*, *31*(41), 14800–14809. doi:10.1523/JNEUROSCI.3231-11.2011

Rotschafer, S. E., Marshak, S., & Cramer, K. S. (2015). Deletion of Fmr1 Alters Function and Synaptic Inputs in the Auditory Brainstem. *Plos One*, *10*(2), e0117266. doi:10.1371/journal.pone.0117266

Rubenstein, J. L. R., & Merzenich, M. M. (2003). Model of autism: increased ratio of excitation/inhibition in key neural systems. *Genes, Brain, and Behavior*, *2*(5), 255–267. doi:10.1046/j.1601-183X.2003.00037.x

Saraga, F., Balena, T., Wolansky, T., Dickson, C. T., & Woodin, M. a. (2008). Inhibitory synaptic plasticity regulates pyramidal neuron spiking in the rodent hippocampus. *Neuroscience*, *155*(1), 64–75. doi:10.1016/j.neuroscience.2008.05.009

Schreiber, S., Fellous, J. M., Whitmer, D., Tiesinga, P., & Sejnowski, T. J. (2003). A new correlation-based measure of spike timing reliability. *Neurocomputing*, *52-54*, 925–931. doi:10.1016/S0925-2312(02)00838-X

Suh, J., Rivest, A. J., Nakashiba, T., Tominaga, T., & Tonegawa, S. (2011). Entorhinal Cortex Layer III Input to the Hippocampus Is Crucial for Temporal Association Memory. *Science (New York, N.Y.)*, (November). doi:10.1126/science.1210125

Tang, X. A., & Alger, B. E. (2015). Homer Protein – Metabotropic Glutamate Receptor Binding Regulates Endocannabinoid Signaling and Affects Hyperexcitability in a Mouse Model of Fragile X Syndrome, *35*(9), 3938–3945. doi:10.1523/JNEUROSCI.4499-14.2015

Tsay, D., Dudman, J. T., & Siegelbaum, S. a. (2007). HCN1 channels constrain synaptically evoked Ca2+ spikes in distal dendrites of CA1 pyramidal neurons. *Neuron*, *56*(6), 1076–89. doi:10.1016/j.neuron.2007.11.015

Turner, D. (1990). Feed-Forward Inhibitory Potentials and Excitatory Interactions in Guinea-Pig Hippocampal Pyramidal Cells. *Journal of Physiology*, *422*(1), 333–350.

Wahlstrom-Helgren, S., & Klyachko, V. A. (2015). GABA $_B$ receptor-mediated feed-forward circuit dysfunction in the mouse model of fragile X syndrome. *The Journal of Physiology*, *0*, n/a–n/a. doi:10.1113/JP271190

Willadt, S., Nenniger, M., & Vogt, K. E. (2013). Hippocampal Feedforward Inhibition Focuses Excitatory Synaptic Signals into Distinct Dendritic Compartments. *PLoS ONE*, *8*(11), e80984. doi:10.1371/journal.pone.0080984

Wlodarczyk, A. I., Xu, C., Song, I., Doronin, M., Wu, Y.-W., Walker, M. C., & Semyanov, A. (2013). Tonic GABAA conductance decreases membrane time constant and increases EPSP-spike precision in hippocampal pyramidal neurons. *Frontiers in Neural Circuits*, *7*(December), 205. doi:10.3389/fncir.2013.00205

Zalay, O. C., & Bardakjian, B. L. (2006). Simulated mossy fiber associated feedforward circuit functioning as a highpass filter. *Conference Proceedings : ... Annual International Conference of the IEEE Engineering in Medicine and Biology Society. IEEE Engineering in Medicine and Biology Society. Conference*, *1*, 4979–82. doi:10.1109/IEMBS.2006.260702

Zhou, M., Tao, H. W., & Zhang, L. I. (2012). Generation of intensity selectivity by differential synaptic tuning: fast-saturating excitation but slow-saturating inhibition. *The Journal of Neuroscience : The Official Journal of the Society for Neuroscience*, *32*(50), 18068–78. doi:10.1523/JNEUROSCI.3647-12.2012